



A mixed formulation of the Bingham fluid flow problem: Analysis and numerical solution

Alexis Aposporidis^{a,*}, Eldad Haber^b, Maxim A. Olshanskii^{c,1}, Alessandro Veneziani^a

^a Department of Mathematics and Computer Science, Emory University, United States

^b Department of Mathematics, University of British Columbia, Canada

^c Department of Mechanics and Mathematics, Moscow M.V. Lomonosov State University, Russia

ARTICLE INFO

Article history:

Received 26 October 2010

Received in revised form 28 February 2011

Accepted 5 April 2011

Available online 12 April 2011

Keywords:

Non-Newtonian flow

Bingham fluid

Mixed formulation

Augmented formulation

Regularization

ABSTRACT

In this paper we introduce a mixed formulation of the Bingham fluid flow problem. We consider both the original and a regularized version of the problem, where a parameter ε is introduced, forcing the entire domain to be formally a fluid region. In general, common solvers for the regularized problem experience a performance degradation when the parameter ε gets smaller. The method studied here introduces an auxiliary tensor variable and shows enhanced numerical properties for small values of ε . A good performance is also observed for the non-regularized case. The well posedness for the regularized problem and the equivalence – at the continuous level – between the original (primitive variables) and the mixed formulation are demonstrated. We analyze properties of linearized problems that are relevant for the convergence of numerical solvers. A finite element method for the mixed formulation is discussed. Numerical results confirm the predicted better performances of the mixed formulation when compared to the primitive variables formulation. A comparison to a non-regularized solver based on the augmented Duvaut–Lions–Glowinski formulation of the problem is carried out as well.

© 2011 Elsevier B.V. All rights reserved.

1. Introduction

The Bingham plastic is a material that behaves like a rigid medium for stresses τ not exceeding a certain critical value τ_s (called the *yield stress*) and behaves like an incompressible fluid if the stresses are equal to or exceed τ_s . The viscosity of the fluid depends on the shear rate, thus the Bingham flow represents an example of a non-Newtonian fluid. Bingham fluids occur in many situations of geophysical as well as industrial interest, see [6] for a comprehensive review, and more recently [37] for the applications in hemodynamics.

Let $D\mathbf{u} = \frac{1}{2}(\nabla\mathbf{u} + \nabla\mathbf{u}^T)$ denote the strain rate tensor and let $|\mathbf{D}\mathbf{u}| = \sqrt{D\mathbf{u} : D\mathbf{u}}$ be the Frobenius norm of $D\mathbf{u}$. The conservation of momentum in the steady case for an incompressible fluid reads

$$\begin{cases} -\operatorname{div}\tau + \nabla p = \mathbf{f} \\ \nabla \cdot \mathbf{u} = 0 \end{cases} \quad \text{in } \Omega, \quad (1.1)$$

where div denotes the divergence operator for tensors, \mathbf{u} , p are the unknown velocity and pressure. For Bingham fluids the domain Ω is split into two subdomains, the fluid region Ω_f and the rigid (or plug) region Ω_r . The constitutive relation for the stress deviator tensor τ and the strain rate tensor reads

$$D\mathbf{u} = \begin{cases} 0 & \text{for } |\tau| \leq \tau_s \text{ (rigid region),} \\ \left(1 - \frac{\tau_s}{|\tau|}\right) \frac{\tau}{2\mu} & \text{for } |\tau| > \tau_s \text{ (fluid region).} \end{cases} \quad (1.2)$$

where the plastic viscosity $\mu > 0$ and the yield stress $\tau_s \geq 0$ are given constants. These equations can be observed as a generalization of the classical Stokes equation having in Ω_f a shear dependent viscosity $\hat{\mu} = 2\mu + \frac{\tau_s}{|D\mathbf{u}|}$ that reduces to the Stokes equations with constant viscosity for $\tau_s = 0$. One of the difficult features of the problem is that the two regions are unknown *a priori* and finding them is a part of the problem; also $\hat{\mu}$ becomes singular in the plug zone. A common way to avoid this difficulty is to regularize $\hat{\mu}$. This can be done in different ways, see e.g., [4,32,18]. Here we consider the Bercovier–Engelman regularization [4]: in the definition of $\hat{\mu}$ the norm $|D\mathbf{u}|$ is replaced with $|D\mathbf{u}|_\varepsilon = \sqrt{D\mathbf{u} : D\mathbf{u} + \varepsilon^2}$. Extension of the approach presented hereafter to other forms of regularization can be considered as well. The regularization ensures $\hat{\mu}$ to be nonsingular even in presence of plug regions and the fluid equations can be posed in the entire domain:

* Corresponding author.

E-mail addresses: aapospo@emory.edu, alexis@aposporidis.com (A. Aposporidis), haber@math.ubc.ca (E. Haber), maxim.olshanskii@mtu-net.ru (M.A. Olshanskii), ale@mathcs.emory.edu (A. Veneziani).

¹ The work of this author was supported in part by the Russian Foundation for Basic Research grants 09-01-00115, 11-01-00971 and by a Visiting Fellowship granted by the Emerson Center for Scientific Computation at Emory University.

$$\begin{cases} -\mathbf{div}\left(2\mu + \frac{\tau_s}{|\mathbf{Du}|_\varepsilon}\right)\mathbf{Du} + \nabla p = \mathbf{f} \\ -\nabla \cdot \mathbf{u} = 0 \end{cases} \quad \text{in } \Omega. \quad (1.3)$$

The regularized model can be treated as the model of a quasi-Newtonian fluid flow and its numerical implementation becomes relatively simple within an existing CFD code. A variety of well-established computational techniques, including parameter free iterative algorithms as Newton method and Krylov subspace methods, can be used to treat the regularized equations numerically. However, the regularization prevents finding the ‘exact’ visco-plastic solution. In particular, finding arrested states and defining plug regions with $\varepsilon > 0$ become non-trivial tasks, see [35] and also [38,39] (the latter papers deal with compressible fluids). Therefore accurate and predictive computations demand using small values of the regularization parameter ε (see e.g., [18,31,12]). Using small values of ε in (1.3) gives rise to several computational issues. For example, the Newton method applied to the regularized problem (1.3) is not robust with respect to ε (see [12] and numerical results in [25,26]). The domain of convergence for the Newton method shrinks as $\varepsilon \rightarrow 0$. Indeed, the norm of the matrix of the second derivatives grows like $O(\varepsilon^{-1})$ [12] implying that to ensure convergence the initial guess for the Newton method should belong to an $O(\varepsilon)$ -neighborhood of the (unknown) solution. One possibility to overcome the issue is to apply a continuation method in ε . This means that ε is selected dynamically and it gets smaller along the iterations. Another option is to perform a number of more robust Picard iterations and switch to the Newton method when a sufficiently good approximation to the solution is found. In the latter case, however, the required number of Picard iterations still grows as $\varepsilon \rightarrow 0$ [25].

Both mathematical and numerical difficulties forced several authors to consider different formulations of the problem (1.1) and (1.2). One approach is based on the variational inequality formulation of Duvaut and Lions [15] and has been proposed by Glowinski and coauthors (see Section 8 of the review paper [13] and refereneces therein). The formulation has been studied mathematically and used to solve the problem numerically with Uzawa-like iterative schemes. The iterations are proven to be convergent upon the introduction of a relaxation parameter (see [12]), however may exhibit a slow convergence rate. Nevertheless, the approach is attractive for solving practical problems when it is necessary to compute the ‘true’ visco-plastic solution and find the plug region (see e.g., [35,34]). We briefly review this approach in Section 5.

In this paper, we consider a different formulation intended to enhance the numerical properties of the regularized formulation (1.3). We introduce an auxiliary symmetric tensor W such that

$$|\mathbf{Du}|_\varepsilon W - \mathbf{Du} = \mathbf{0}. \quad (1.4)$$

Equations (1.3) in Ω with the auxiliary variable read

$$\begin{cases} -\mathbf{div}(2\mu\mathbf{Du} + \tau_s W) + \nabla p = \mathbf{f}, \\ -\nabla \cdot \mathbf{u} = 0. \end{cases} \quad (1.5)$$

System (1.4) and (1.5) represents the mixed formulation we investigate in this paper. We will show that this formulation is efficient for solving the regularized problem. For a given ε the number of nonlinear iterations required for convergence is significantly reduced compared to solving the original problem (1.3) in the primitive variables. While most analysis of (1.4) and (1.5) is carried out in this paper for $\varepsilon > 0$, numerical results show that the method remains efficient even for the case $\varepsilon = 0$. In this case, the approach and the resulting iterative method compares favorably with the Uzawa type algorithm for the augmented Lagrangian saddle-point formulation of Glowinski et al.

The mixed formulation (1.4) and (1.5) is closely related with the approach of Cea and Glowinski [7] (see also Sections 5–7 in [13]). In that approach a symmetric tensor W satisfying $W : \mathbf{Du} = |\mathbf{Du}|$ was introduced in the numerical formulation through the relation

$$W = \mathbf{P}(W + r\mathbf{Du}) \quad \forall r \geq 0, \quad (1.6)$$

with the projector \mathbf{P} on the convex set of tensor functions $Z \in (L^2(\Omega))^{d \times d}$ satisfying $|Z| < 1$. The projector is defined by $\mathbf{P}(Z)(\mathbf{x}) := Z(\mathbf{x})[\max\{1, |Z(\mathbf{x})|\}]^{-1}$. The equations (1.5) and (1.6) were solved numerically with the Uzawa type method with W serving for the primal iterated variable and r as a relaxation parameter. Further, a special regularization was introduced in [13] to facilitate the application of a variant of the Newton method. While formulation (1.4) and (1.5) is formally equivalent to (1.5) and (1.6) for $\varepsilon = 0$, it leads to a different variational formulation and finite element solutions, coupled iterative algorithms of Picard and (for $\varepsilon > 0$) Newton may be directly applied. Moreover (1.4) and (1.5) is amenable to common regularizations like the one used in this paper.

The remainder of the paper is organized as follows. Necessary notations and preliminaries are given in Section 1.1. In Section 2, we consider the weak formulations of (1.3) and (1.4)–(1.5) and prove some well-posedness results. Some linearized problems are studied here as well. We prove that the weak formulations of (1.3) and (1.4)–(1.5) are equivalent in the sense that they share the unique solution. At the same time, equivalence does not necessarily hold for the corresponding numerical discretizations. In Section 3 we introduce non-linear iterative methods of Picard and Newton for solving (1.3) and (1.4)–(1.5). Several convergence estimates for the case $\varepsilon > 0$ are proven which suggest the superior properties of (1.4) and (1.5) in building efficient solvers. A finite element discretization method is considered in Section 4, including the discussion of algebraic properties of resulting discrete systems. In Section 5 we briefly recall another method for numerical treatment of the Bingham problem (1.1) based on variational inequalities and augmentation. Several numerical results are presented in Section 6. These results show that the mixed formulation (1.4) and (1.5) leads to much better convergence rates than the primitive variables formulation (1.3). Moreover, it appears that the Picard method for solving (1.4) and (1.5) is applicable with $\varepsilon = 0$ and demonstrates fast convergence even in this limit case. Thus for $\varepsilon = 0$, we include few results of comparison with the Uzawa method for the augmented saddle-point formulation of Glowinski et al. In this section, we also consider a continuation Newton method based on the mixed formulation. Section 7 contains some closing remarks.

1.1. Notations and preliminaries

In what follows, we use the standard notation for the functional spaces we need: for $1 \leq p \leq \infty$ and $k > 0$, $L^p(\Omega)$, $H^k(\Omega)$ are standard Lebesgue and Sobolev spaces. Also $L^2_0(\Omega)$ denotes the subspace of $L^2(\Omega)$ of functions with zero mean over Ω , $H^1_0(\Omega)$ is the space of functions in $H^1(\Omega)$ with vanishing trace on $\partial\Omega$. The corresponding spaces for (2D or 3D) vectors are denoted in bold, e.g. $\mathbf{L}^2(\Omega)$, $\mathbf{H}^k(\Omega)$ or $\mathbf{H}^1_0(\Omega)$. The subspace of $\mathbf{H}^1_0(\Omega)$ of divergence free vector-functions is denoted by \mathbf{V} . We use the notation $\mathcal{H}^k(\Omega)$ for tensors whose components are $H^k(\Omega)$ functions. For symmetric tensors, this particularizes to $\mathcal{S}^p_s(\Omega)$, $\mathcal{H}^k_s(\Omega)$. When there is no possibility of confusion, we omit the indication of the domain Ω . The norm in H^k is denoted by $\|\cdot\|_k$, the scalar product and the norm in L^2 is denoted by (\cdot, \cdot) and $\|\cdot\|$, respectively, the same norm and product notation is used for the vector and tensor counterparts of H^k and L^2 .

From the vector identities $2\mathbf{div}D = \Delta + \nabla \nabla \cdot$ and $\nabla \nabla \cdot = \Delta + \nabla \times \nabla \times$ with the help of integration by parts one immediately gets the following Korn type inequalities

$$\|D\mathbf{u}\| \leq \|\nabla\mathbf{u}\| \leq \sqrt{2}\|D\mathbf{u}\| \quad \forall \mathbf{u} \in \mathbf{H}_0^1, \tag{1.7}$$

stating the equivalence between the L^2 norms of the gradient and its symmetric part. We shall also refer to the Friedrichs inequality

$$\|\mathbf{u}\| \leq C_F \|\nabla\mathbf{u}\| \quad \forall \mathbf{u} \in \mathbf{H}_0^1. \tag{1.8}$$

2. Some well-posedness results for the regularized problem

We assume that the domain is polygonal or $\partial\Omega \in \mathcal{C}^{1,1}$ and that $\mathbf{f} \in \mathbf{L}^2$. Moreover, for the sake of analysis, we assume homogeneous Dirichlet boundary conditions to hold (i.e. $\mathbf{u} = \mathbf{0}$ on $\partial\Omega$). The generalization to mixed Dirichlet/Neumann boundary problems is straightforward.

Our primary goal is to develop and study a formulation of the regularized Bingham problem with enhanced robustness properties with respect to a small regularization parameter. Thus, if not explicitly stated otherwise, we consider further only the regularized version of the problem, i.e. $\varepsilon > 0$. However, we shall also address some properties of the problem for $\varepsilon \rightarrow 0$.

Let us introduce the following bilinear forms,

$$a(\mathbf{u}, \mathbf{v}) = \int_{\Omega} 2\mu D\mathbf{u} : D\mathbf{v} \quad \text{on } \mathbf{H}_0^1 \times \mathbf{H}_0^1,$$

$$b(p, \mathbf{v}) = - \int_{\Omega} p \nabla \cdot \mathbf{v} \quad \text{on } L_0^2 \times \mathbf{H}_0^1.$$

For the form

$$a_{\varepsilon}(\mathbf{u}, \mathbf{v}) := a(\mathbf{u}, \mathbf{v}) + \int_{\Omega} \frac{\tau_s}{|D\mathbf{u}|_{\varepsilon}} D\mathbf{u} : D\mathbf{v} \quad \text{on } \mathbf{H}_0^1 \times \mathbf{H}_0^1,$$

one readily checks (thanks to the Korn and the Friedrichs inequalities (1.7) and (1.8) the coercivity

$$a_{\varepsilon}(\mathbf{u}, \mathbf{u}) \geq c \|\mathbf{u}\|_1^2 \quad \forall \mathbf{u} \in \mathbf{H}_0^1 \tag{2.1}$$

and continuity

$$a_{\varepsilon}(\mathbf{u}, \mathbf{v}) \leq \left(2\mu + \frac{\tau_s}{\varepsilon}\right) \|\mathbf{u}\|_1 \|\mathbf{v}\|_1 \quad \forall \mathbf{u}, \mathbf{v} \in \mathbf{H}_0^1. \tag{2.2}$$

Moreover, one can show the strict monotonicity:

$$a_{\varepsilon}(\mathbf{u}, \mathbf{u} - \mathbf{v}) - a_{\varepsilon}(\mathbf{v}, \mathbf{u} - \mathbf{v}) \geq c \|\mathbf{u} - \mathbf{v}\|_1^2 \quad \forall \mathbf{u}, \mathbf{v} \in \mathbf{H}_0^1. \tag{2.3}$$

Indeed, it holds

$$\begin{aligned} a_{\varepsilon}(\mathbf{u}, \mathbf{u} - \mathbf{v}) - a_{\varepsilon}(\mathbf{v}, \mathbf{u} - \mathbf{v}) &= \int_{\Omega} 2\mu |D\mathbf{u} - D\mathbf{v}|^2 + \tau_s \left(\frac{D\mathbf{u} - D\mathbf{v}}{|D\mathbf{u}|_{\varepsilon}} \right. \\ &\quad \left. + \left(\frac{1}{|D\mathbf{u}|_{\varepsilon}} - \frac{1}{|D\mathbf{v}|_{\varepsilon}} \right) D\mathbf{v} \right) : (D\mathbf{u} - D\mathbf{v}) = \int_{\Omega} 2\mu |D\mathbf{u} - D\mathbf{v}|^2 \\ &\quad + \frac{\tau_s}{|D\mathbf{u}|_{\varepsilon}} \left(|D\mathbf{u} - D\mathbf{v}|^2 - \frac{|D\mathbf{u}|_{\varepsilon} - |D\mathbf{v}|_{\varepsilon}}{|D\mathbf{v}|_{\varepsilon}} D\mathbf{v} : (D\mathbf{u} - D\mathbf{v}) \right) \\ &\geq \int_{\Omega} 2\mu |D\mathbf{u} - D\mathbf{v}|^2 + \frac{\tau_s}{|D\mathbf{u}|_{\varepsilon}} \left(|D\mathbf{u} - D\mathbf{v}|^2 - \frac{|D\mathbf{u} - D\mathbf{v}|}{|D\mathbf{v}|_{\varepsilon}} D\mathbf{v} : (D\mathbf{u} - D\mathbf{v}) \right). \end{aligned}$$

Monotonicity (2.3) follows from (1.7) applied to the first term in the last inequality and noting that since $\|D\mathbf{v}\|_{\varepsilon}^{-1} D\mathbf{v} \leq 1$, the second term is non-negative.

The weak formulation of the regularized problem (1.3) reads: find $\mathbf{u} \in \mathbf{H}_0^1$, $p \in L_0^2$ such that for any $\mathbf{v} \in \mathbf{H}_0^1$, $q \in L_0^2$

$$a_{\varepsilon}(\mathbf{u}, \mathbf{v}) - b(p, \mathbf{v}) + b(q, \mathbf{u}) = (\mathbf{f}, \mathbf{v}). \tag{2.4}$$

Proposition 1. *The problem (2.4) has a unique solution $\{\mathbf{u}, p\} \in \mathbf{H}_0^1 \times L_0^2$ satisfying the estimate*

$$\|\nabla\mathbf{u}\| \leq \mu^{-1} \|\mathbf{f}\|_{-1}, \quad \|p\| \leq c(\|\mathbf{f}\|_{-1} + \tau_s \min\{1, \varepsilon^{-1}\} \|\mathbf{f}\|_{-1}). \tag{2.5}$$

Proof. First, consider (2.4) restricted to the divergence-free subspace \mathbf{V} : find $\mathbf{u} \in \mathbf{V}$ such that

$$a_{\varepsilon}(\mathbf{u}, \mathbf{v}) = (\mathbf{f}, \mathbf{v}) \quad \forall \mathbf{v} \in \mathbf{V}. \tag{2.6}$$

Thanks to (2.1)–(2.3) and $\mathbf{V} \subset \mathbf{H}_0^1$ one applies the Browder–Minty method of strictly monotone operators (see e.g., [16], Section 9.1) to prove the existence and uniqueness of $\mathbf{u} \in \mathbf{V}$ solving (2.6). The equivalence of (2.6) and (2.4) together with the existence and uniqueness of the pressure as a Lagrange multiplier corresponding to the div-free constraint can be shown by a standard argument, see [23]. To prove the estimate (2.5) for velocity one sets in (2.4) $\mathbf{v} = \mathbf{u}$ and $q = p$ and applies the $(\mathbf{f}, \mathbf{v}) \leq \|\mathbf{f}\|_{-1} \|\nabla\mathbf{v}\|$ inequality to estimate the right-hand side. The bound for the pressure follows thanks to the Nečas inequality

$$\|p\| \leq c \sup_{\mathbf{v} \in \mathbf{H}_0^1} \frac{(\nabla \cdot \mathbf{v}, p)}{\|\nabla\mathbf{v}\|}. \tag{2.7}$$

Indeed, setting in (2.4) $q = 0$, dividing the equality by $\|\nabla\mathbf{v}\|$ and exploiting $\|D\mathbf{u}\|_{\varepsilon}^{-1} D\mathbf{u} < 1$ and the Korn and Cauchy inequalities one obtains

$$\begin{aligned} \frac{(\nabla \cdot \mathbf{v}, p)}{\|\nabla\mathbf{v}\|} &= \frac{2\mu(D\mathbf{u}, D\mathbf{v}) + \tau_s(|D\mathbf{u}|_{\varepsilon}^{-1} D\mathbf{u}, D\mathbf{v}) - (\mathbf{f}, \mathbf{v})}{\|\nabla\mathbf{v}\|} \\ &\leq \frac{2\mu\|\nabla\mathbf{u}\| \|\nabla\mathbf{v}\| + \tau_s(1, |D\mathbf{v}|) + \|\mathbf{f}\|_{-1} \|\nabla\mathbf{v}\|}{\|\nabla\mathbf{v}\|} \\ &\leq 2\mu\|\nabla\mathbf{u}\| + \tau_s|\Omega|^{\frac{1}{2}} + \|\mathbf{f}\|_{-1}. \end{aligned}$$

Passing to the upper limit with respect to \mathbf{v} and using (2.7) yields

$$\|p\| \leq c(2\mu\|\nabla\mathbf{u}\| + \tau_s|\Omega|^{\frac{1}{2}} + \|\mathbf{f}\|_{-1}).$$

The estimate

$$\|p\| \leq c\left(2\mu + \frac{\tau_s}{\varepsilon}\right) \|\nabla\mathbf{u}\| + \|\mathbf{f}\|_{-1}.$$

is proven by the same arguments through the use of (2.2). Combining both estimates leads to the pressure estimate in (2.5). \square

Notice that for the limit case $\varepsilon = 0$ we do not have the implication $\mathbf{f} \rightarrow 0 \Rightarrow p \rightarrow 0$ because in the model the kinematic pressure is under-determined in the rigid zone.

To handle the mixed form (1.4) and (1.5) we define the following bilinear and non-linear forms

$$\begin{aligned} c(\mathbf{u}, Z) &= \int_{\Omega} \tau_s D\mathbf{u} : Z \quad \text{on } \mathbf{H}_0^1 \times \mathcal{L}_s^2, \quad g(|D\mathbf{u}|_{\varepsilon}, W, Z) = \int_{\Omega} \tau_s |D\mathbf{u}| W \\ &\quad : Z \quad \text{on } \mathbf{H}_0^1 \times \mathcal{L}_s^2 \times \mathcal{L}_s^{\infty}. \end{aligned}$$

Note that $g(|D\mathbf{u}|_{\varepsilon}, W, Z)$ is well defined on $\mathbf{H}_0^1 \times \mathcal{L}_s^2 \times \mathcal{L}_s^{\infty}$ and it holds

$$|g(|D\mathbf{u}|_{\varepsilon}, W, Z)| \leq \|\mathbf{u}\|_1 \|W\| \|Z\|_{L^{\infty}}.$$

The weak formulation of (1.4) and (1.5) reads as follows: Find $\mathbf{u} \in \mathbf{H}_0^1$, $p \in L_0^2$ and $W \in \mathcal{L}_s^2$ such that for any $\mathbf{v} \in \mathbf{H}_0^1$, $q \in L_0^2$ and $Z \in \mathcal{L}_s^{\infty}$

$$\begin{aligned} a(\mathbf{u}, \mathbf{v}) - b(p, \mathbf{v}) + c(\mathbf{v}, W) + b(q, \mathbf{u}) + c(\mathbf{u}, Z) \\ - g(|D\mathbf{u}|_{\varepsilon}, W, Z) \\ = (\mathbf{f}, \mathbf{v}). \end{aligned} \tag{2.8}$$

Now we are in position to prove the following well-posedness result:

Theorem 1. *The problem (2.8) has a unique solution $\{\mathbf{u}, W, p\}$ from $\mathbf{H}_0^1 \times \mathcal{L}_s^2 \times L_0^2$ such that*

$$\begin{aligned} \|\mathbf{u}\|_1^2 + \varepsilon\tau_s \|W\|^2 &\leq \|\mathbf{f}\|_{-1}, \quad \|p\| \\ &\leq c(\|\mathbf{f}\|_{-1} + \tau_s \min\{1, \varepsilon^{-1}\} \|\mathbf{f}\|_{-1}). \end{aligned} \tag{2.9}$$

Moreover $W \in \mathcal{L}_s^{\infty}$ and

$$\|W\|_{L^{\infty}} \leq 1. \tag{2.10}$$

Proof. The proof of the well-posedness is based on showing the equivalence of (2.8) and (2.4) and applying Proposition 1. Indeed, assume \mathbf{u}, p from $\mathbf{H}_0^1 \times L_0^2$ solves (2.4) and define $W := |\mathbf{D}\mathbf{u}|_\varepsilon^{-1} \mathbf{D}\mathbf{u}$. Since $\mathbf{D}\mathbf{u} \in \mathcal{L}_s^2$ we conclude that the components of W are measurable functions (as products of such functions). Moreover, since for any $\mathbf{x} \in \Omega$, $\|\mathbf{D}\mathbf{u}(\mathbf{x})|_\varepsilon^{-1} \mathbf{D}\mathbf{u}(\mathbf{x})\| \leq 1$, we have $W \in \mathcal{L}_s^\infty$ and both equalities $W|\mathbf{D}\mathbf{u}|_\varepsilon^{-1} = \mathbf{D}\mathbf{u}$ and $W = |\mathbf{D}\mathbf{u}|_\varepsilon^{-1} \mathbf{D}\mathbf{u}$ hold in \mathcal{L}_s^2 . Therefore, in view of (2.4) and noting that for $W = |\mathbf{D}\mathbf{u}|_\varepsilon^{-1} \mathbf{D}\mathbf{u}$ it holds

$$a(\mathbf{u}, \mathbf{v}) + c(\mathbf{v}, W) = a_\varepsilon(\mathbf{u}, \mathbf{v}),$$

we conclude that the triple $\{\mathbf{u}, W, p\}$ satisfies (2.8) for any $\{\mathbf{v}, Z, q\}$ from $\mathbf{H}_0^1 \times \mathcal{L}_s^\infty \times L_0^2$. Thus the existence of a solution to (2.8) follows from Proposition 1. Now assume that some $\{\mathbf{u}, W, p\}$ solves (2.8). Setting $\mathbf{v} = 0, q = 0$ and varying $Z \in \mathcal{L}_s^\infty$ we conclude that $|\mathbf{D}\mathbf{u}|_\varepsilon W = \mathbf{D}\mathbf{u}$ holds in $(\mathcal{L}_s^\infty)' \equiv \mathcal{L}_s^1$. Hence for any solution of (2.8) it holds

$$W = |\mathbf{D}\mathbf{u}|_\varepsilon^{-1} \mathbf{D}\mathbf{u} \quad \text{a.e.} \quad (2.11)$$

Using this in the third term of (2.8) and setting $Z = 0$ we deduce that \mathbf{u}, p satisfy (2.4). The uniqueness of the solution to (2.8) follows from Propositions 1 and 2.11. Finally, the first two estimates in (2.9) follow by the same arguments as in (2.5), i.e. by taking $\mathbf{v} = \mathbf{u}, q = p, Z = W$, and $W \in \mathcal{L}_s^\infty$ with (2.10) follows from (2.11). \square

Although the formulations (2.8) and (2.4) are equivalent, their (finite element) discretizations are *not necessarily equivalent* and feature different numerical properties.

We are not aware of possible extensions of the results of Theorem 1 or Proposition 1 to the limit case of $\varepsilon = 0$. Some well-posedness results for the (non-regularized) Bingham problem are based on the reformulation of the problem as a variational inequality, see [15]. In [2] a non-regularized nonhomogeneous problem is analyzed as a limit case of a regularized problem with an existence result for 2D periodic problems. Somewhat related results can be found in [5], where the Navier–Stokes unsteady equations are considered for fluids featuring a stress tensor of the form

$$\boldsymbol{\tau} = \mu(\delta + |\mathbf{D}\mathbf{u}|)^{s-2} \mathbf{D}\mathbf{u}, \quad s \in (1, \infty).$$

The extension to the case $s = 1$ and to the Bingham fluid problem is still an open problem.

Remark 1. Once we proved that the solution W of (2.8) is actually from \mathcal{L}_s^∞ one can extend the space of admissible test functions Z in (2.8) from \mathcal{L}_s^∞ to \mathcal{L}_s^2 .

The mixed formulation and convex programming. The velocity solution to the Bingham problem (1.1) satisfies

$$\mathbf{u} = \arg \min_{\mathbf{v} \in \mathbf{V}} \mathcal{J}(\mathbf{v}),$$

where the functional $\mathcal{J}(\cdot)$ reads $\mathcal{J}(\mathbf{v}) = \mu \|\mathbf{D}\mathbf{v}\|^2 + \tau_s \int_\Omega |\mathbf{D}\mathbf{v}| - \int_\Omega \mathbf{f}\mathbf{v}$. Notice that

$$\int_\Omega |\mathbf{D}\mathbf{v}| = \sup_{|W| \leq 1} \int_\Omega \mathbf{D}\mathbf{v} : W \quad \text{for } \mathbf{v} \in \mathbf{H}_0^1.$$

By the duality theory for convex programming, the mixed formulation (1.4) and (1.5) can be observed therefore as the Euler–Lagrange system corresponding to the saddle point problem

$$\min_{\mathbf{v} \in \mathbf{V}} \sup_{|W| \leq 1} \left\{ \mu \|\mathbf{D}\mathbf{v}\|^2 + \tau_s \int_\Omega \mathbf{D}\mathbf{v} : W - \int_\Omega \mathbf{f}\mathbf{v} \right\}.$$

This introduces W from (1.4) as a dual variable. The argument has been advocated in [11] for an image restoration problem and gave additional stimulus to the present work. In that paper, the scalar variable u is the grey-level of an image and the minimization involves the total variation $\int_\Omega |\nabla u|$. The analogies between image restoration problems and visco-plastic fluids have been already exploited in [19,20].

3. Iterative methods

3.1. Two auxiliary linear problems

Let $\boldsymbol{\beta} \in \mathbf{H}_0^1$ be given, we look for \mathbf{u}, p such that

$$\begin{cases} -\operatorname{div} \left(\left(2\mu + \frac{\tau_s}{|\mathbf{D}\boldsymbol{\beta}|_\varepsilon} \right) \mathbf{D}\mathbf{u} \right) + \nabla p = \mathbf{f} & \text{in } \Omega \\ \nabla \cdot \mathbf{u} = 0 \end{cases} \quad (3.1)$$

with $\mathbf{u} = \mathbf{0}$ on $\partial\Omega$ for simplicity. Let us introduce the bilinear form on $\mathbf{V} \times \mathbf{V}$,

$$a_\beta(\mathbf{u}, \mathbf{v}) := \int_\Omega \left(2\mu + \frac{\tau_s}{|\mathbf{D}\boldsymbol{\beta}|_\varepsilon} \right) \mathbf{D}\mathbf{u} : \mathbf{D}\mathbf{v}.$$

The weak formulation of (3.1) reads: find $(\mathbf{u}, p) \in \mathbf{H}_0^1 \times L_0^2$ such that

$$a_\beta(\mathbf{u}, \mathbf{v}) + b(p, \mathbf{v}) - b(q, \mathbf{u}) = (\mathbf{f}, \mathbf{v}) \quad \forall (\mathbf{v}, q) \in \mathbf{H}_0^1 \times L_0^2. \quad (3.2)$$

The following proposition can be promptly proven:

Proposition 2. Given $\mathbf{f} \in \mathbf{L}^2$ and $\boldsymbol{\beta} \in \mathbf{H}_0^1$, there exists a unique solution $\{\mathbf{u}, p\}$ to (3.2).

Proof. Thanks to the Korn and Friedrichs inequality, the bilinear form $a_\beta(\cdot, \cdot)$ is coercive,

$$a_\beta(\mathbf{u}, \mathbf{u}) \geq \mu \|\nabla \mathbf{u}\|^2 \geq c \|\mathbf{u}\|_1^2.$$

It is also straightforward to check that $a_\beta(\cdot, \cdot)$ is continuous on $\mathbf{V} \times \mathbf{V}$. Since \mathbf{V} can be equivalently defined as $\mathbf{V} := \{\mathbf{v} \in \mathbf{H}_0^1 : b(q, \mathbf{v}) = 0 \forall q \in L_0^2\}$, the result of the Proposition follows from Corollary 5.1 from [23]. \square

The mixed formulation of (3.1) reads

$$\begin{cases} -\operatorname{div}(2\mu \mathbf{D}\mathbf{u} + W) + \nabla p = \mathbf{f} \\ \nabla \cdot \mathbf{u} = 0 \\ |\mathbf{D}\boldsymbol{\beta}|_\varepsilon W - \mathbf{D}\mathbf{u} = 0 \end{cases} \quad \text{in } \Omega. \quad (3.3)$$

Denote $g_{\varepsilon, \beta}(W, Z) \equiv \int_\Omega \tau_s |\mathbf{D}\boldsymbol{\beta}|_\varepsilon W : Z$. The weak form of (3.3) reads: find $\{\mathbf{u}, p, W\} \in \mathbf{H}_0^1 \times L_0^2 \times \mathcal{L}_s^2$ such that

$$a(\mathbf{u}, \mathbf{v}) + b(p, \mathbf{v}) + c(\mathbf{v}, W) - b(q, \mathbf{u}) - c(\mathbf{u}, Z) + g_{\varepsilon, \beta}(W, Z) = (\mathbf{f}, \mathbf{v}) \quad (3.4)$$

for any $(\mathbf{v}, q, Z) \in \mathbf{H}_0^1 \times L_0^2 \times \mathcal{L}_s^\infty$.

Proposition 3. Given $\mathbf{f} \in \mathbf{L}^2$ and $\boldsymbol{\beta} \in \mathbf{V}$, there exists a unique solution $\{\mathbf{u}, p, W\}$ to (3.4).

Proof. The proof is carried out by showing the equivalence of the primitive variables and mixed weak formulations (3.2) and (3.4) and then applying Proposition 2. The arguments are largely the same as in the nonlinear case, see the proof of Theorem 1. The solution of (3.2) $\{\mathbf{u}, p\}$ together with $W := |\mathbf{D}\boldsymbol{\beta}|_\varepsilon^{-1} \mathbf{D}\mathbf{u} \in \mathcal{L}_s^2$ solves (3.4). Reverse implication: if $\{\mathbf{u}, p, W\}$ solves (3.2), then setting $\mathbf{v} = 0, q = 0$ and varying $Z \in \mathcal{L}_s^\infty$ one finds that $|\mathbf{D}\boldsymbol{\beta}|_\varepsilon^{-1} W = \mathbf{u}$ holds in $(\mathcal{L}_s^\infty)' \equiv \mathcal{L}_s^1$. Thus $W = |\mathbf{D}\boldsymbol{\beta}|_\varepsilon^{-1} \mathbf{D}\mathbf{u}$ holds almost everywhere in Ω . Inserting this in the third term of (3.4) and letting $Z=0$ we find that \mathbf{u}, p solves (3.2). \square

On the numerical level, problem (3.2) or (3.3) has to be solved at each iteration of the Picard algorithm for (1.3) or (1.4) and (1.5), respectively.

3.2. Picard iteration

Given the well-posedness results for the auxiliary linear problems (3.1) and (3.3) we now consider iterative methods of Picard

type to iterate for the solutions of nonlinear problems (1.3)–(1.5). For the original problem (1.3) one iteration reads: given $\mathbf{u}^{(k)} \in \mathbf{H}_0^1$, find $\mathbf{u}^{(k+1)} \in \mathbf{H}_0^1$, $p^{(k+1)} \in L_0^2$ such that

$$\begin{cases} -\mathbf{div}\left(2\mu + \frac{\tau_s}{|\mathbf{Du}^{(k)}|_\varepsilon}\right)\mathbf{Du}^{(k+1)} + \nabla p^{(k+1)} = \mathbf{f}, \\ -\nabla \cdot \mathbf{u}^{(k+1)} = 0. \end{cases} \quad (3.5)$$

Likewise, for the mixed problem (1.4) and (1.5) one iteration reads: given $\mathbf{u}^{(k)} \in \mathbf{H}_0^1$, find $\mathbf{u}^{(k+1)} \in \mathbf{H}_0^1$, $p^{(k+1)} \in L_0^2$, $W^{(k+1)} \in \mathcal{L}^2$ such that

$$\begin{cases} -\mathbf{div}(2\mu\mathbf{Du}^{(k+1)} + \tau_s W^{(k+1)}) + \nabla p^{(k+1)} = \mathbf{f}, \\ -\nabla \cdot \mathbf{u}^{(k+1)} = 0, \\ |\mathbf{Du}^{(k)}|_\varepsilon W^{(k+1)} - \mathbf{Du}^{(k+1)} = \mathbf{0}. \end{cases} \quad (3.6)$$

These problem are of the form (3.1) and (3.3) with $\beta = \mathbf{u}^{(k)}$ and $\mathbf{u} = \mathbf{u}^{(k+1)}$ and should be understood in the weak sense of (3.2) and (3.4). Thus, due to Propositions 2 and 3 a single Picard iteration is well-defined.

3.2.1. Analysis of the Picard iterations

Denote by \mathbf{u}, p, W the solution to (2.8) (\mathbf{u}, p also solve (2.4) and $\mathbf{e}^{(k)} \equiv \mathbf{u}^{(k)} - \mathbf{u}$, $E^{(k)} \equiv W^{(k)} - W$ and $e^{(k)} \equiv p^{(k)} - p$). Consider first the iterations (3.5) for the original formulation of the problem (2.4). Eqs. (2.4) and (3.5) yield the following error equation

$$a(\mathbf{e}^{(k+1)}, \mathbf{v}) + \int_\Omega \tau_s \left(\frac{\mathbf{Du}^{(k+1)}}{|\mathbf{Du}^{(k)}|_\varepsilon} - \frac{\mathbf{Du}}{|\mathbf{Du}|_\varepsilon} \right) : \mathbf{Dv} + b(\mathbf{v}, e^{(k+1)}) - b(\mathbf{e}^{(k+1)}, q) = 0, \quad (3.7)$$

for all $\mathbf{v} \in \mathbf{V}$ and $q \in L_0^2$.

Proposition 4. The velocity error of the iteration (3.5) satisfies

$$\|\mathbf{e}^{(k+1)}\|_1 \leq C\varepsilon^{-1}\|\mathbf{e}^{(k)}\|_1 + O\left(\|\mathbf{e}^{(k)}\|_1^2\right). \quad (3.8)$$

Proof. We rewrite the second term in (3.7) as

$$\begin{aligned} & \int_\Omega \tau_s \left(\frac{\mathbf{Du}^{(k+1)}}{|\mathbf{Du}^{(k)}|_\varepsilon} - \frac{\mathbf{Du}}{|\mathbf{Du}^{(k)}|_\varepsilon} + \frac{\mathbf{Du}}{|\mathbf{Du}^{(k)}|_\varepsilon} - \frac{\mathbf{Du}}{|\mathbf{Du}|_\varepsilon} \right) : \mathbf{Dv} \\ &= \int_\Omega \tau_s \frac{\mathbf{De}^{(k+1)}}{|\mathbf{Du}^{(k)}|_\varepsilon} : \mathbf{Dv} + \int_\Omega \tau_s \left(\frac{1}{|\mathbf{Du}^{(k)}|_\varepsilon} - \frac{1}{|\mathbf{Du}|_\varepsilon} \right) \mathbf{Du} : \mathbf{Dv}. \end{aligned}$$

Upon Fréchet linearization, which is always possible for $\varepsilon > 0$, we have

$$\frac{1}{|\mathbf{Du}^{(k)}|_\varepsilon} - \frac{1}{|\mathbf{Du}|_\varepsilon} = \frac{\mathbf{Du} : \mathbf{De}^{(k)}}{|\mathbf{Du}|_\varepsilon^3} + \text{h.o.t.} \quad (3.9)$$

Let us now select $\mathbf{v} = \mathbf{e}^{(k+1)}$ and $q = e^{(k+1)}$ in the error Eq. (3.7), so that we have

$$\begin{aligned} a(\mathbf{e}^{(k+1)}, \mathbf{e}^{(k+1)}) + \int_\Omega \tau_s \frac{\mathbf{De}^{(k+1)} : \mathbf{De}^{(k+1)}}{|\mathbf{Du}^{(k)}|_\varepsilon} \\ = - \int_\Omega \tau_s \left(\frac{\mathbf{Du} : \mathbf{De}^{(k)}}{|\mathbf{Du}|_\varepsilon^3} + \text{h.o.t.} \right) \mathbf{Du} : \mathbf{De}^{(k+1)}. \end{aligned} \quad (3.10)$$

Exploiting the coercivity of the bilinear form $a(\cdot, \cdot)$, inequality (1.7), the bound (2.9) on \mathbf{u} (independent of ε) and noting that $\frac{x^2}{\sqrt{(x^2+\varepsilon^2)^3}} \leq \frac{2}{27}\varepsilon^{-1}$ for any $x \in \mathbb{R}$, we obtain the inequality

$$\mu\|\nabla\mathbf{e}^{(k+1)}\|^2 \leq \frac{C}{\varepsilon} \left(\|\mathbf{e}^{(k)}\|_1 + O\left(\|\mathbf{e}^{(k)}\|_1^2\right) \right) \|\mathbf{e}^{(k+1)}\|_1 \quad (3.11)$$

where C here and after is a constant independent of ε . The latter inequality yields (3.8). \square

The previous theorem quantifies the impact of small values of the regularization parameter ε on the Picard iteration in the primitive variables formulation. In general, small values of ε slow down the convergence, as was mentioned in the introduction and pointed out in [25,26].

Let us consider now a similar analysis for the mixed formulation.

Proposition 5. The error of the iteration (3.6) satisfies

$$\|\mathbf{e}^{(k+1)}\|_1 + \varepsilon^{\frac{1}{2}}\|E^{(k+1)}\| \leq C\varepsilon^{-\frac{1}{2}}\|\mathbf{e}^{(k)}\|_1. \quad (3.12)$$

Proof. After a memberwise subtraction of (3.6) and (4.1) and standard manipulations with $\mathbf{v} = \mathbf{e}^{(k+1)}$, $q = e^{(k+1)}$ and $Z = E^{(k+1)}$ (test function can be taken from \mathcal{L}_s^2 , cf. Remark 1), we get

$$\begin{aligned} a(\mathbf{e}^{(k+1)}, \mathbf{e}^{(k+1)}) + g_\varepsilon\left(|\mathbf{Du}^{(k)}|_\varepsilon - |\mathbf{Du}|_\varepsilon, W, E^{(k+1)}\right) \\ + g_\varepsilon\left(|\mathbf{Du}^{(k)}|_\varepsilon, E^{(k+1)}, E^{(k+1)}\right) = 0. \end{aligned} \quad (3.13)$$

For the mapping $f(\mathbf{v}) := |\mathbf{Dv}|_\varepsilon$ from \mathbf{H}^1 to L^2 we find the Fréchet derivative operator

$$d(f)|_{\mathbf{a}} = |\mathbf{Da}|_\varepsilon^{-1}\mathbf{Da} : D \Rightarrow \|d(f)|_{\mathbf{a}}\|_{\mathbf{H}_0^1 \rightarrow L^2} \leq 1 \quad \forall \mathbf{a} \in \mathbf{H}_0^1. \quad (3.14)$$

Therefore it holds

$$\|\mathbf{Du}^{(k)}|_\varepsilon - |\mathbf{Du}|_\varepsilon\| \leq \|\mathbf{De}^{(k)}\|. \quad (3.15)$$

Recalling $\|W\|_{L^\infty} \leq 1$ (cf. Theorem 1) and $g_\varepsilon(|\mathbf{Du}^{(k)}|_\varepsilon, E^{(k+1)}, E^{(k+1)}) \geq \varepsilon\|E^{(k+1)}\|^2$, we obtain from (3.13) and (3.15) the inequality

$$\begin{aligned} \mu\|\nabla\mathbf{e}^{(k+1)}\|_1^2 + \varepsilon\|E^{(k+1)}\|^2 &\leq \tau_s\|\mathbf{e}^{(k)}\|_1\|E^{(k+1)}\| \\ &\leq \frac{\tau_s^2}{2\varepsilon}\|\mathbf{e}^{(k)}\|_1^2 + \frac{\varepsilon}{2}\|E^{(k+1)}\|^2. \end{aligned} \quad (3.16)$$

Thus we get

$$\|\mathbf{e}^{(k+1)}\|_1^2 + \varepsilon\|E^{(k+1)}\|^2 \leq C\tau_s^2\varepsilon^{-1}\|\mathbf{e}^{(k)}\|_1^2. \quad \square$$

Remark 2. Notice that (3.12) enjoys a milder dependence on ε than (3.8); also the higher order terms disappear. At the same time, the velocity (and pressure) iterations from (3.5) and (3.6) are the same (thanks to the equivalence of the auxiliary linear systems discussed in Section 3.1). Thus the velocity error $\mathbf{e}^{(k)}$ from (3.5) should also satisfy the improved bound (3.12). However, the argument to show this improved bound is indirect and resorts to the mixed formulation. Moreover, such an indirect argument may not be valid in the discrete case, since the equivalence does not necessarily hold any longer, apart from some special choice of the discretization scheme (see Section 6). Testing both formulations numerically shows that iterative methods for the mixed one are less sensitive to small values of ε .

A relaxed formulation. The method of the previous section can be generalized by introducing a relaxation parameter $\vartheta \in [0, 1]$. If \mathbf{u}^* denotes the solution to (3.5) or (3.6), we set

$$\mathbf{u}^{(k+1)} = \vartheta\mathbf{u}^* + (1 - \vartheta)\mathbf{u}^{(k)}.$$

Relaxation can be either static or dynamic, i.e. with ϑ depending on k .

Given $\beta \in \mathbf{H}_0^1$ define the following norms:

$$\begin{aligned} \|\mathbf{u}\|_\beta &:= \left(\|\nabla\mathbf{u}\|^2 + \tau_s\|D\beta|_\varepsilon^{-\frac{1}{2}}\mathbf{Du}\|^2 \right)^{\frac{1}{2}} \quad \text{on } \mathbf{H}_0^1, \\ \|\mathbf{u}, W\|_\beta &:= \left(\|\nabla\mathbf{u}\|^2 + \tau_s\|D\beta|_\varepsilon^{-\frac{1}{2}}W\|^2 \right)^{\frac{1}{2}} \quad \text{on } \mathbf{H}_0^1 \times \mathcal{L}_s^\infty. \end{aligned} \quad (3.17)$$

We prove the following theorem.

Theorem 2. *The relaxed versions of the Picard iterations (3.5) and (3.6) admit the following error reduction relations:*

$$\begin{aligned} \text{for (3.5)} \quad & \| \mathbf{e}^{(k+1)} \|_{\mathbf{u}^{(k)}} \leq (1 - c\varepsilon^2) \| \mathbf{e}^{(k)} \|_{\mathbf{u}^{(k)}} + O(\| \mathbf{e}^{(k)} \|_{\mathbf{u}^{(k)}}^3), \quad \text{with } \vartheta = c\varepsilon^2, \\ \text{for (3.6)} \quad & \| \mathbf{e}^{(k+1)}, \mathbf{E}^{(k+1)} \|_{\mathbf{u}^{(k)}} \leq (1 - c\varepsilon) \| \mathbf{e}^{(k)}, \mathbf{E}^{(k)} \|_{\mathbf{u}^{(k)}}, \quad \text{with } \vartheta = c\varepsilon, \end{aligned} \quad (3.18)$$

and sufficiently small positive constant c independent of ε .

Proof. The proof of the first estimate in (3.18) is a simple variation of the arguments used in proving Proposition 4. We show the proof below. The error equation reads (compare to (3.7))

$$\begin{aligned} a(\mathbf{e}^{(k+1)} - (1 - \vartheta)\mathbf{e}^{(k)}, \mathbf{v}) + \int_{\Omega} \tau_s \vartheta \left(\frac{D\mathbf{u}^*}{|D\mathbf{u}^{(k)}|_{\varepsilon}} - \frac{D\mathbf{u}}{|D\mathbf{u}|_{\varepsilon}} \right) : D\mathbf{v} \\ + b(\mathbf{v}, e^{(k+1)}) - b(\mathbf{e}^{(k+1)}, q) = 0, \end{aligned} \quad (3.19)$$

for all $\mathbf{v} \in \mathbf{V}$ and $q \in Q$. To produce the last term on the left-hand side of (3.19) we use that $\mathbf{u}^{(k)}, \mathbf{u}^* \in \mathbf{V}$ yields $\mathbf{u}^{(k+1)} \in \mathbf{V}$. We rewrite the second term in (3.19) as

$$\begin{aligned} \int_{\Omega} \vartheta \tau_s \left(\frac{D\mathbf{u}^*}{|D\mathbf{u}^{(k)}|_{\varepsilon}} - \frac{D\mathbf{u}}{|D\mathbf{u}^{(k)}|_{\varepsilon}} + \frac{D\mathbf{u}}{|D\mathbf{u}^{(k)}|_{\varepsilon}} - \frac{D\mathbf{u}}{|D\mathbf{u}|_{\varepsilon}} \right) : D\mathbf{v} \\ = \int_{\Omega} \tau_s \frac{D(\mathbf{e}^{(k+1)} - (1 - \vartheta)\mathbf{e}^{(k)})}{|D\mathbf{u}^{(k)}|_{\varepsilon}} : D\mathbf{v} \\ + \vartheta \int_{\Omega} \tau_s \left(\frac{1}{|D\mathbf{u}^{(k)}|_{\varepsilon}} - \frac{1}{|D\mathbf{u}|_{\varepsilon}} \right) D\mathbf{u} : D\mathbf{v}. \end{aligned}$$

Set $\mathbf{v} = \mathbf{e}^{(k+1)}$ and $q = e^{(k+1)}$ in Eq. (3.19) and use (3.9) to obtain

$$\begin{aligned} a(\mathbf{e}^{(k+1)} - (1 - \vartheta)\mathbf{e}^{(k)}, \mathbf{e}^{(k+1)}) + \int_{\Omega} \tau_s \frac{D(\mathbf{e}^{(k+1)} - (1 - \vartheta)\mathbf{e}^{(k)})}{|D\mathbf{u}^{(k)}|_{\varepsilon}} : D\mathbf{e}^{(k+1)} \\ = -\vartheta \int_{\Omega} \tau_s \left(\frac{D\mathbf{u} : D\mathbf{e}^{(k)}}{|D\mathbf{u}|_{\varepsilon}^3} + \text{h.o.t.} \right) D\mathbf{u} : D\mathbf{e}^{(k+1)} \\ = -\vartheta \int_{\Omega} \tau_s \left(\frac{D\mathbf{u} : D\mathbf{e}^{(k)}}{|D\mathbf{u}|_{\varepsilon}^3} + \text{h.o.t.} \right) D\mathbf{u} : (D\mathbf{e}^{(k+1)} - (1 - \vartheta)D\mathbf{e}^{(k)}) \\ - \vartheta(1 - \vartheta) \int_{\Omega} \tau_s \frac{(D\mathbf{u} : D\mathbf{e}^{(k)})^2}{|D\mathbf{u}|_{\varepsilon}^3} + O(\| \mathbf{e}^{(k)} \|_1^3). \end{aligned} \quad (3.20)$$

Now we note that the second integral term on the right-hand side of (3.20) is negative, exploit the simple identity $2(a - b, a) = \|a\|^2 - \|b\|^2 + \|a - b\|^2$ as well as $\frac{x^2}{\sqrt{(x^2 + \varepsilon^2)^3}} \leq \frac{2}{\sqrt{27}} \varepsilon^{-1}$ and the Cauchy inequality to obtain the inequality

$$\begin{aligned} \| \mathbf{e}^{(k+1)} \|_{\mathbf{u}^{(k)}}^2 + \| \mathbf{e}^{(k+1)} - (1 - \vartheta)\mathbf{e}^{(k)} \|_{\mathbf{u}^{(k)}}^2 \leq (1 - \vartheta)^2 \| \mathbf{e}^{(k)} \|_{\mathbf{u}^{(k)}}^2 \\ + \frac{C}{\varepsilon} \vartheta \| D\mathbf{e}^{(k)} \| \| D(\mathbf{e}^{(k+1)} - (1 - \vartheta)\mathbf{e}^{(k)}) \| + O(\| \mathbf{e}^{(k)} \|_1^3) \end{aligned}$$

with C independent of ε . Now we apply the Young inequality to the handle the second term on the right-hand side and get after a cancellation

$$\| \mathbf{e}^{(k+1)} \|_{\mathbf{u}^{(k)}}^2 \leq (1 - \vartheta)^2 \| \mathbf{e}^{(k)} \|_{\mathbf{u}^{(k)}}^2 + \frac{C^2}{4\varepsilon^2} \vartheta^2 \| D\mathbf{e}^{(k)} \|^2 + O(\| \mathbf{e}^{(k)} \|_1^3).$$

The latter inequality proves the first estimate in (3.18) for $\vartheta = c\varepsilon^2$, with a sufficiently small positive constant c independent of ε . Similar changes should be applied to the arguments of Proposition 5 to show the second estimate in (3.18). \square

We note that the error norms in (3.18) depend in general on the iteration number k . Thus we consider (3.18) as an error reduction property rather than a convergence result. However, comparing the reduction factors for both formulations we note that the mixed formulation still leads to a milder dependence on ε than the original one.

3.3. The Newton method

For the primitive variables formulation (1.3) one step of the Newton method can be written as follows: given $\mathbf{u}^{(k)}$ find $\mathbf{u}^{(k+1)}$, $p^{(k+1)}$ solving

$$\begin{aligned} -\text{div} \left(2\mu + \frac{\tau_s}{|D\mathbf{u}^{(k)}|_{\varepsilon}} \left[1 - \frac{D\mathbf{u}^{(k)} D\mathbf{u}^{(k)}}{|D\mathbf{u}^{(k)}|_{\varepsilon}^2} \right] \right) D\mathbf{u}^{(k+1)} + \nabla p^{(k+1)} = \mathbf{f} - \tau_s \text{div} \frac{D\mathbf{u}^{(k)} |D\mathbf{u}^{(k)}|^2}{|D\mathbf{u}^{(k)}|_{\varepsilon}^3}, \\ \nabla \cdot \mathbf{u}^{(k+1)} = 0. \end{aligned} \quad (3.21)$$

For the mixed formulation one step of the Newton method reads: given $\mathbf{u}^{(k)}, W^{(k)}$ find $\mathbf{u}^{(k+1)}, p^{(k+1)}, W^{(k+1)}$ solving

$$\begin{aligned} -\text{div} \left(2\mu D\mathbf{u}^{(k+1)} + \tau_s W^{(k+1)} \right) + \nabla p^{(k+1)} = \mathbf{f}, \\ \nabla \cdot \mathbf{u}^{(k+1)} = 0, \\ D\mathbf{u}^{(k+1)} - |D\mathbf{u}^{(k)}|_{\varepsilon} W^{(k+1)} - \frac{D\mathbf{u}^{(k)} : D\mathbf{u}^{(k+1)}}{|D\mathbf{u}^{(k)}|_{\varepsilon}} W^{(k)} = - \frac{|D\mathbf{u}^{(k)}|^2}{|D\mathbf{u}^{(k)}|_{\varepsilon}} W^{(k)}. \end{aligned} \quad (3.22)$$

As stated in the Introduction, the degradation of performance of the Newton method when ε gets smaller can be remedied in different ways. One possibility is to use a *mix of Picard and Newton methods*: One performs a few iterations of more robust Picard method and starts Newton when a good initial guess becomes available. Another possibility is a *continuation strategy* that corresponds to a non-stationary selection of ε , such that $\varepsilon = \varepsilon(k)$ and $\lim_{k \rightarrow \infty} \varepsilon(k) = 0$. Numerical results with these strategies will be presented in Section 6.

Remark 3. While the Picard iterations formally produce the same approximations for velocity and pressure for both formulations, cf. Remark 2, the Newton method approximations are in general *different* for primitive variables and mixed formulations *both* on continuous and discrete levels. This can be seen by eliminating $W^{(k+1)}$ from (3.22) with the help of the third relation. Doing this one finds that (3.21) and (3.22) would be equivalent only if $W^{(k)} = |D\mathbf{u}^{(k)}|_{\varepsilon}^{-1} D\mathbf{u}^{(k)}$. The latter is not expected to be true for a general k , since setting $W^{(k)} = |D\mathbf{u}^{(k)}|_{\varepsilon}^{-1} D\mathbf{u}^{(k)}$ in (3.22) does not imply $W^{(k+1)} = |D\mathbf{u}^{(k+1)}|_{\varepsilon}^{-1} D\mathbf{u}^{(k+1)}$. Numerical experience shows that for small values of ε (3.22) is considerably less sensitive to the choice of the initial guess than (3.21).

4. Finite element approximation

There are different ways to discretize (1.1), examples are the MAC discretization on staggered grids and collocated finite difference methods [27,30], finite volume [36] or LBB-stable finite elements [13]. In this paper we consider Galerkin finite element discretization methods, although the approach is essentially independent of a specific discretization method.

Denote by $\mathbf{H}_h \subset \mathbf{H}_0^1$, $Q_h \subset L_0^2$ and $\mathcal{W}_h \subset \mathcal{L}_s^2$ the finite dimensional subspaces for the velocity, pressure and W , respectively. We assume that the pair of spaces \mathbf{H}_h, Q_h is LBB stable [23]. The finite element method for (2.8) reads: find $\mathbf{u}_h \in \mathbf{H}_h$, $p_h \in Q_h$, $W_h \in \mathcal{W}_h$ such that

$$\begin{aligned} a(\mathbf{u}_h, \mathbf{v}_h) + b(p_h, \mathbf{v}_h) + c(\mathbf{v}_h, W_h) - b(q_h, \mathbf{u}_h) - c(\mathbf{u}_h, Z_h) \\ + g_{\varepsilon}(\mathbf{u}_h, W_h, Z_h) = (\mathbf{f}, \mathbf{v}_h) \end{aligned} \quad (4.1)$$

for any $\mathbf{v}_h \in \mathbf{H}_h$, $q_h \in Q_h$ and $Z_h \in \mathcal{W}_h$.

Now we address the well-posedness and stability of (4.1). Unlike the continuous case (see Theorem 1) the discrete problem (4.1) is not in general equivalent to the finite element counterpart of the original problem (2.4). Thus the well-posedness for (4.1) would not follow directly from the theory of monotone operators applied to the Galerkin formulation of (2.4). The proof of the

well-posedness for (4.1) relies on the Schaefer’s extension of the Brouwer theorem (a.k.a. the Leray-Schauder theorem, see e.g., [16], Sections 8.1.4 and 9.2.2).

Theorem 3. *The problem (4.1) has a solution $\{\mathbf{u}_h, W_h, p_h\}$ from $\mathbf{H}_h \times W_h \times Q_h$ such that*

$$\|\mathbf{u}_h\|_1^2 + \varepsilon \tau_s \|W_h\|_0^2 \leq \|\mathbf{f}\|_{-1}, \quad \|p_h\| \leq c(1 + \tau_s \varepsilon^{-1}) \|\mathbf{f}\|_{-1}. \quad (4.2)$$

If f is sufficiently small or μ, ε are sufficiently large then the solution is unique.

Proof. Define the discrete divergence-free space $\mathbf{V}_h := \{\mathbf{v}_h \in \mathbf{H}_h : b(q_h, \mathbf{v}_h) = 0 \ \forall q_h \in Q_h\}$. For arbitrary $\lambda \in [0, 1]$ consider the problem: find $\mathbf{u}_h^\lambda \in \mathbf{V}_h, W_h^\lambda \in \mathcal{W}_h$ such that

$$\begin{aligned} a(\mathbf{u}_h^\lambda, \mathbf{v}_h) + \lambda c(\mathbf{v}_h, W_h^\lambda) &= \lambda(\mathbf{f}, \mathbf{v}_h), \\ g_\varepsilon(\mathbf{u}_h^\lambda, W_h^\lambda, Z_h) - \lambda c(\mathbf{u}_h^\lambda, Z_h) &= 0, \end{aligned} \quad (4.3)$$

for any $\mathbf{v}_h \in \mathbf{V}_h$ and $Z_h \in \mathcal{W}_h$. For $\lambda = 1$ the problem (4.3) is equivalent to (4.1). To apply the Leray-Schauder fixed point theorem it is sufficient to show: (i) the set of solutions to (4.3) is bounded uniformly with respect to λ and (ii) the mapping $\{\mathbf{u}_h^{\text{old}}, W_h^{\text{old}}\} \rightarrow \{\mathbf{u}_h^{\text{new}}, W_h^{\text{new}}\}$ defined by

$$\begin{aligned} a(\mathbf{u}_h^{\text{new}}, \mathbf{v}_h) &= (\mathbf{f}, \mathbf{v}_h) - c(\mathbf{v}_h, W_h^{\text{old}}) \quad \forall \mathbf{v}_h \in \mathbf{V}_h, \\ g_\varepsilon(\mathbf{u}_h^{\text{old}}, W_h^{\text{new}}, Z_h) &= c(\mathbf{u}_h^{\text{old}}, Z_h) \quad \forall Z_h \in \mathcal{W}_h \end{aligned} \quad (4.4)$$

is continuous and bounded (all spaces are of finite dimension, so the boundedness implies compactness).

To find a bound for $\mathbf{u}_h^\lambda, W_h^\lambda$ we set in (4.3) $\mathbf{v}_h = \mathbf{u}_h^\lambda, Z_h = W_h^\lambda$. Summing up the equalities gives

$$\begin{aligned} \min(2\mu, \tau_s \varepsilon) (\|\nabla \mathbf{u}_h^\lambda\|^2 + \|W_h^\lambda\|^2) \\ \leq a(\mathbf{u}_h^\lambda, \mathbf{u}_h^\lambda) + g_\varepsilon(\mathbf{u}_h^\lambda, W_h^\lambda, W_h^\lambda) = \lambda(\mathbf{f}, \mathbf{u}_h^\lambda) \\ \leq \frac{1}{2} \min(2\mu, \tau_s \varepsilon) \|\nabla \mathbf{u}_h^\lambda\|^2 + \max(\mu^{-1}, \tau_s^{-1} \varepsilon^{-1}) \|\mathbf{f}\|_{-1}^2. \end{aligned}$$

Thus

$$\|\nabla \mathbf{u}_h^\lambda\|^2 + \|W_h^\lambda\|^2 \leq \max(\mu^{-2}, \tau_s^{-2} \varepsilon^{-2}) \|\mathbf{f}\|_{-1}^2 \quad \forall \lambda \in [0, 1].$$

Now we check that the mapping defined by (4.4) is bounded and continuous. To see the boundedness we set in (4.4) $\mathbf{v}_h = \mathbf{u}_h^{\text{new}}, Z_h = W_h^{\text{new}}$ and get through the Cauchy and Friedrichs inequalities:

$$\|\nabla \mathbf{u}_h^{\text{new}}\| \leq c(\tau_s \|W_h^{\text{old}}\| + \|\mathbf{f}\|_{-1}) \quad \text{and} \quad \varepsilon \|W_h^{\text{new}}\| \leq \|\nabla \mathbf{u}_h^{\text{old}}\|.$$

The continuity follows from the observation that forms in (4.4) are continuous with respect to every argument. Hence the Leray-Schauder theorem provides the existence of a solution to (4.3) for $\lambda = 1$. Let \mathbf{u}_1, W_1 and \mathbf{u}_2, W_2 be two solutions to (4.3) with $\lambda = 1$. Denote $\mathbf{e} = \mathbf{u}_1 - \mathbf{u}_2$ and $E = W_1 - W_2$. One sets $\mathbf{v}_h = \mathbf{e}$ and $Z_h = E$ in (4.3) and readily gets

$$2\mu \|\mathbf{De}\|^2 + g_\varepsilon(\mathbf{u}_1, E, E) + (g_\varepsilon(\mathbf{u}_1, W_2, E) - g_\varepsilon(\mathbf{u}_2, W_2, E)) = 0. \quad (4.5)$$

Thus (4.5) and (3.14) yields

$$2\mu \|\mathbf{De}\|^2 + \varepsilon \|E\|^2 - \|W_2\|_{L^\infty} \|\mathbf{De}\| \|E\| \leq 0.$$

Now the a priori bound (4.2) and the smallness assumption yield the uniqueness result. The standard argument [23] shows the existence and uniqueness of the pressure p_h as a Lagrange multiplier. \square

Even though the equivalence between primitive variables and mixed formulation at the discrete level does not necessarily hold, in Section 6 we will consider a particular selection of finite element subspaces that ensures this equivalence to hold.

4.1. Algebraic properties

Denote by N_{vel}, N_p and N_w the number of degrees of the freedom of each velocity component in \mathbf{H}_h , the pressure in Q_h and each component of the symmetric tensors in \mathcal{W}_h , respectively. Let $\{\varphi_i\}$ for $i = 1, \dots, N_{vel}$ be the basis functions for each velocity component, $\{q_i\}$ for $i = 1, \dots, N_p$ the basis functions of Q_h , and $\{z_i\}$ for $i = 1, \dots, N_w$ the basis functions for each entry of the symmetric tensors. We introduce to the following notation for 2D problems²: Matrix A is $2N_{vel} \times 2N_{vel}$ s.t.

$$A = \begin{bmatrix} A^{11} & A^{12} \\ A^{21} & A^{22} \end{bmatrix}, \quad \begin{cases} A_{ij}^{11} = \int_\Omega \mu \left(\frac{\partial \varphi_j}{\partial x_1} \frac{\partial \varphi_i}{\partial x_1} + \frac{1}{2} \frac{\partial \varphi_j}{\partial x_2} \frac{\partial \varphi_i}{\partial x_2} \right), \\ A_{ij}^{12} = A_{ji}^{21} = \int_\Omega \mu \frac{\partial \varphi_j}{\partial x_1} \frac{\partial \varphi_i}{\partial x_2}, \\ A_{ij}^{22} = \int_\Omega \mu \left(\frac{\partial \varphi_j}{\partial x_2} \frac{\partial \varphi_i}{\partial x_2} + \frac{1}{2} \frac{\partial \varphi_j}{\partial x_1} \frac{\partial \varphi_i}{\partial x_1} \right). \end{cases} \quad (4.6)$$

Matrix B is $2N_{vel} \times N_p$ s.t.

$$B = [B^1 \ B^2], \quad B_{ij}^1 = - \int_\Omega q_i \frac{\partial \varphi_j}{\partial x_1}, \quad B_{ij}^2 = - \int_\Omega q_i \frac{\partial \varphi_j}{\partial x_2}. \quad (4.7)$$

We assume that the finite elements for velocity and pressure are inf-sup compatible, so that B^T is a full-rank matrix.³

Matrix C is $2N_{vel} \times 3N_w$ s.t.

$$C = \begin{bmatrix} C^{1,1} & C^{2,1} & C^{12,1} \\ C^{1,2} & C^{2,2} & C^{12,2} \end{bmatrix}, \quad \begin{cases} C_{ij}^{1,1} = \int_\Omega \tau_s z_j \frac{\partial \varphi_i}{\partial x_1}, \quad C^{2,1} = 0, \quad C_{ij}^{12,1} = \int_\Omega \tau_s z_j \frac{\partial \varphi_i}{\partial x_2}, \\ C^{1,2} = 0, \quad C_{ij}^{2,2} = \int_\Omega \tau_s z_j \frac{\partial \varphi_i}{\partial x_2}, \quad C_{ij}^{12,2} = \int_\Omega \tau_s z_j \frac{\partial \varphi_i}{\partial x_1}. \end{cases} \quad (4.8)$$

Finally, we define matrix $N \in \mathbb{R}^{3N_w \times 3N_w}$ s.t.

$$N = \text{blockdiag}(N^1, N^2, N^{12}), \quad N_{ij}^l = \int_\Omega \tau_s |D\mathbf{u}_h^{(k)}|_{\varepsilon} z_j z_i, \quad l = 1, 2, 3. \quad (4.9)$$

Notice that N is a weighted type mass matrix, so in computations it can often be replaced by a lumped (diagonal) matrix.

Each iteration of the Picard method for the mixed formulation requires solving a system of the form

$$\mathcal{A} \begin{bmatrix} \mathbf{U} \\ \mathbf{W} \\ \mathbf{P} \end{bmatrix} = \begin{bmatrix} \mathbf{b} \\ \mathbf{0} \\ \mathbf{0} \end{bmatrix}, \quad \text{with } \mathcal{A} = \begin{bmatrix} A & C & B^T \\ C^T & -N & \mathbf{0} \\ B & \mathbf{0} & \mathbf{0} \end{bmatrix}. \quad (4.10)$$

and $\mathbf{U} = [U_1; U_2]^T, \mathbf{W} = [W_1, W_2, W_{12}]^T$ and \mathbf{P} are the vectors of the nodal values of the unknowns. Let us denote for convenience

$$\mathfrak{D} = \begin{bmatrix} A & C \\ C^T & -N \end{bmatrix}, \quad \mathfrak{B} = [B \ \mathbf{0}], \quad \text{then } \mathcal{A} = \begin{bmatrix} \mathfrak{D} & \mathfrak{B}^T \\ \mathfrak{B} & \mathbf{0} \end{bmatrix}.$$

Proposition 6. *For $\varepsilon > 0$, system (4.10) is non-singular for any choice of the finite element subspace \mathcal{W}_h .*

Proof. First we prove that \mathfrak{D} is non-singular. To this end, consider the matrix factorization

$$\mathfrak{D} = \begin{bmatrix} I & \mathbf{0} \\ C^T A^{-1} & I \end{bmatrix} \begin{bmatrix} A & \mathbf{0} \\ \mathbf{0} & \Sigma_w \end{bmatrix} \begin{bmatrix} I & A^{-1} C \\ \mathbf{0} & I \end{bmatrix},$$

with Schur complement matrix $\Sigma_w = -(A^{-1} + CN^{-1}C^T)$. Thus \mathfrak{D} is non-singular if N and Σ_w are non-singular. Since $\varepsilon > 0, N$ is invertible. The non-singularity of Σ_w follows from the observation that

² In 3D we have 3 velocity components and 6 different components of the tensor W .

³ If we impose $\mathbf{u} = 0$ on the entire boundary $\partial\Omega$, then B is one-rank deficient having hydrostatic pressure mode in its kernel. This will however not alter our further considerations.

```

 $\gamma_h := \gamma_h^{(0)}, \tau_h := \tau_h^{(0)} \in \mathcal{W}_h;$ 
while (convergence == false)
    find  $[\mathbf{u}_h, p_h]$  solution to  $\begin{cases} \int_{\Omega} \lambda D\mathbf{u}_h : D\mathbf{v}_h + b(p_h, \mathbf{v}_h) = \frac{1}{2} \int_{\Omega} (\tau_h - 2\lambda\gamma_h) : D\mathbf{v}_h + (\mathbf{f}, \mathbf{v}_h), \\ b(q_h, \mathbf{u}_h) = 0. \end{cases}$ 
     $\gamma_h := \begin{cases} 0 & \text{if } |\tau_h + 2\lambda D\mathbf{u}_h| \leq \tau_s, \\ \left(1 - \frac{\tau_s}{|\tau_h + 2\lambda D\mathbf{u}_h|}\right) \frac{\tau_h + 2\lambda D\mathbf{u}_h}{2(\lambda + \mu)} & \text{otherwise.} \end{cases}$ 
     $\tau_h := \tau_h + 2\lambda(D\mathbf{u}_h - \gamma_h).$ 
    test(convergence)
end
    
```

Fig. 5.1. Uzawa scheme for the Lions–Glowinski augmented formulation.

A and N are symmetric positive definite. By the same argument, \mathcal{A} is non-singular if \mathfrak{D} and the Schur complement $\mathfrak{B}\mathfrak{D}^{-1}\mathfrak{B}^T$ are non-singular. For the pressure Schur complement of \mathcal{A} we get

$$-\mathfrak{B}\mathfrak{D}^{-1}\mathfrak{B}^T = -B\Sigma_W^{-1}B^T,$$

which is a symmetric positive definite matrix, so the proposition is proven. \square

For $\varepsilon = 0$, the previous result does not hold and the non-singularity of the system is not guaranteed. A necessary condition in this case is that $\text{Ker}(C) \cap \text{Ker}(N) = \emptyset$. The question of the selection of finite dimensional spaces forcing the well posedness of the discrete problem in this case is open.

5. The Lions–Glowinski augmented formulation

In [24] an alternative variational formulation is considered. To underline differences and similarities with our approach we briefly recall the method from [24]. The solution of the Bingham problem (1.1) \mathbf{u}, τ together with γ is the saddle point of the following Lagrangian:

$$\begin{aligned} \mathcal{L}(\mathbf{u}; \gamma; \tau) = & \mu \int_{\Omega} |\gamma|^2 dx + \tau_s \int_{\Omega} |\gamma| dx + \int_{\Omega} (\mathbf{D}(\mathbf{u}) - \gamma) : \tau dx \\ & + \lambda \int_{\Omega} |\mathbf{D}(\mathbf{u}) - \gamma|^2 dx - \int_{\Omega} \mathbf{f} \cdot \mathbf{u} dx. \end{aligned}$$

Here $\lambda \geq 0$ is an auxiliary augmentation parameter. Then

$$\mathcal{L}(\mathbf{u}, \gamma, \tau) = \min_{\sigma \in \mathcal{L}_s^2, \mathbf{v} \in \mathbf{V}} \max_{\xi \in \mathcal{L}_s^2} \mathcal{L}(\mathbf{v}; \sigma; \xi). \tag{5.1}$$

Note that the auxiliary variable γ is introduced in a way that $\gamma = D\mathbf{u}$ in a weak sense. This is in contrast to our approach where $|D\mathbf{u}|^{-1}D\mathbf{u}$ is treated as the auxiliary variable W .

The variational saddle point problem (5.1) can be equivalently written as an integral inequality problem, see Duvaut and Lions [15]. For $\varepsilon > 0$, however, one can also look for the equivalent integral equality formulation. In our notation it would read: find \mathbf{u}, p and γ such that

$$\begin{aligned} \lambda a(\mathbf{u}, \mathbf{v}) + b(p, \mathbf{v}) + \frac{1}{2}c(\tau - 2\lambda\gamma, \mathbf{v}) &= (\mathbf{f}, \mathbf{v}), \\ b(q, \mathbf{u}) &= 0, \\ c(\psi, \mathbf{u}) - (\gamma, \psi) &= 0, \\ \tau &= 2\mu\gamma + \tau_s\gamma|\gamma|_e. \end{aligned}$$

for any test functions \mathbf{v}, q, ψ in appropriate spaces. Departing from this formulation, different discretization schemes can be considered. We note that the penalty parameter λ also plays the role of the relaxation parameter in the iterative algorithm of Uzawa type. In [24] the iterative algorithm (further referred as **ALG**) for solving (5.1) is considered, see Fig. 5.1.

The convergence can be tested using different stopping criteria. Here we consider the difference between $\tau_h^{(k+1)}$ and $\tau_h^{(k)}$, that basically means that we test the residual $D\mathbf{u}_h^{(k)} - \gamma_h^{(k)}$. One of the strong aspects of this scheme is that it does not require a regularization parameter $\varepsilon > 0$ and the method is proven to be convergent. However, no convergence rate has been rigorously established and the numerical evidence suggests that convergence can be very slow. We include some numerical results with this approach in the next section.

6. Numerical results

In this section we present results of several numerical experiments illustrating the performance of the approach introduced in the paper. We compare the results with the primitive variables formulation and show an advantage in using the mixed formulation, especially for small values of ε . A few experiments with the mixed formulation are done for the non-regularized case ($\varepsilon = 0$). In this case its performance is compared with the **ALG** algorithm for the Lions–Glowinski augmented formulation. We will also consider the Newton continuation method and give numerical evidence of its effectiveness. Finally, we will show some results for domains with a less trivial geometry.

6.1. Primal vs mixed, quadrilateral elements

In this first set of experiments we use the IFISS package in MATLAB [17]. Problem (1.5) is discretized using Q2–Q1 finite elements for velocity and pressure, respectively, and the mixed variable W is discretized in Q1. Starting with the zero vector as an initial guess, we perform Picard iterations until $\frac{\|\mathbf{r}_k\|_{\infty}}{\|\mathbf{r}_0\|_{\infty}} \leq 10^{-6}$, i.e. until the initial residual drops by six orders of magnitude. Unless stated otherwise, $\mu = 1$ and $\mathbf{f} = \mathbf{0}$. MATLAB’s backslash operator serves as the linear solver. Note that when ε gets smaller the linear systems are expected to become increasingly ill-conditioned (for both primitive variables and mixed form) and *ad hoc* preconditioned iterative method should be developed to solve them efficiently for mid-size and larger problems.

In practice, another good initial guess is given by the solution of a Stokes (Newtonian) problem.

6.1.1. An Analytical Test Case

One of the few available analytical solutions to (1.1) describes the flow between two parallel plates, and in two dimensions it is given by

$$u_1 = \begin{cases} \frac{1}{8}[(1 - 2\tau_s)^2 - (1 - 2\tau_s - 2y)^2], & \text{if } 0 \leq y < \frac{1}{2} - \tau_s, \\ \frac{1}{8}(1 - 2\tau_s)^2, & \text{if } \frac{1}{2} - \tau_s \leq y \leq \frac{1}{2} + \tau_s, \\ \frac{1}{8}[(1 - 2\tau_s)^2 - (2y - 2\tau_s - 1)^2], & \text{if } \frac{1}{2} + \tau_s < y \leq 1, \end{cases} \tag{6.1}$$

Table 6.1

Number of Picard iterations required for reducing the residual of a factor 10^{-6} in the analytical test case for $\tau_s = 0.3$ and different h and ε in both primitive variables and mixed formulation. The last column shows results for the non-regularized case (that is not working in the primitive variables formulation).

$h \setminus \varepsilon \rightarrow$	10^{-1}	10^{-2}	10^{-3}	10^{-4}	10^{-5}	10^{-1}	10^{-2}	10^{-3}	10^{-4}	10^{-5}	0
	Primitive variables					Mixed variables					
1 / 16	7	20	15	30	38	5	12	17	20	23	19
1 / 32	7	23	60	81	83	4	12	19	24	25	24
1 / 64	7	27	89	95	88	4	9	14	16	16	22
1 / 128	6	23	61	134	192	3	8	11	12	12	13

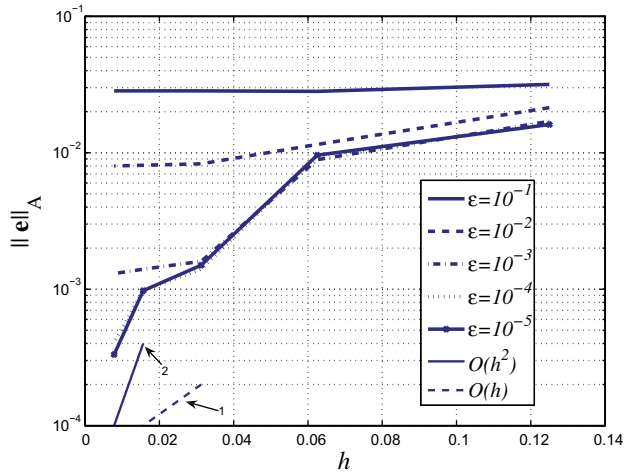


Fig. 6.1. Numerical error $\|\mathbf{u} - \mathbf{u}_{ex}\|_A = \sqrt{(\mathbf{u} - \mathbf{u}_{ex})^T A (\mathbf{u} - \mathbf{u}_{ex})}$ for different sizes of the mesh and different ε . The matrix A is a finite element stiffness matrix. The thin solid line is a reference line for $O(h^2)$, the thin dotted one is for $O(h)$.

$u_2 \equiv 0$ and $p = -x$. The rigid region $\{y \in \Omega | \frac{1}{2} - \tau_s \leq y \leq \frac{1}{2} + \tau_s\}$ is the kernel moving at a constant velocity. In our experiment, we choose $\tau_s = 0.3$. We impose Dirichlet boundary conditions on the domain $\Omega = [0, 1]^2$ according to (6.1). The number of Picard iterations for both primitive variables and mixed formulations can be seen in Table 6.1. The comparison clearly outlines the advantage of using the mixed formulation. In particular, we noticed that even for the non-regularized case the mixed formulation is convergent and gets accurate results.

Fig. 6.1 shows the numerical error in the discrete energy norm for different choices of ε and h (obtained with the mixed formulation). For the analytical velocity solution \mathbf{u} from (6.1) it holds $\mathbf{u} \in \mathbf{H}^2$, but $\mathbf{u} \notin \mathbf{H}^3$. This limits the guaranteed order of convergence to $O(h)$ in the energy norm. Large values of ε with small values of h clearly prevent the optimal convergence rate of the finite element method. For smaller values of ε the observed order of convergence is between 1 and 2.

Fig. 6.2, top left, shows the computed pressure field. The pressure field indicates a numerical error in the area around the rigid region. This is expected, since in the model the stress tensor is un-

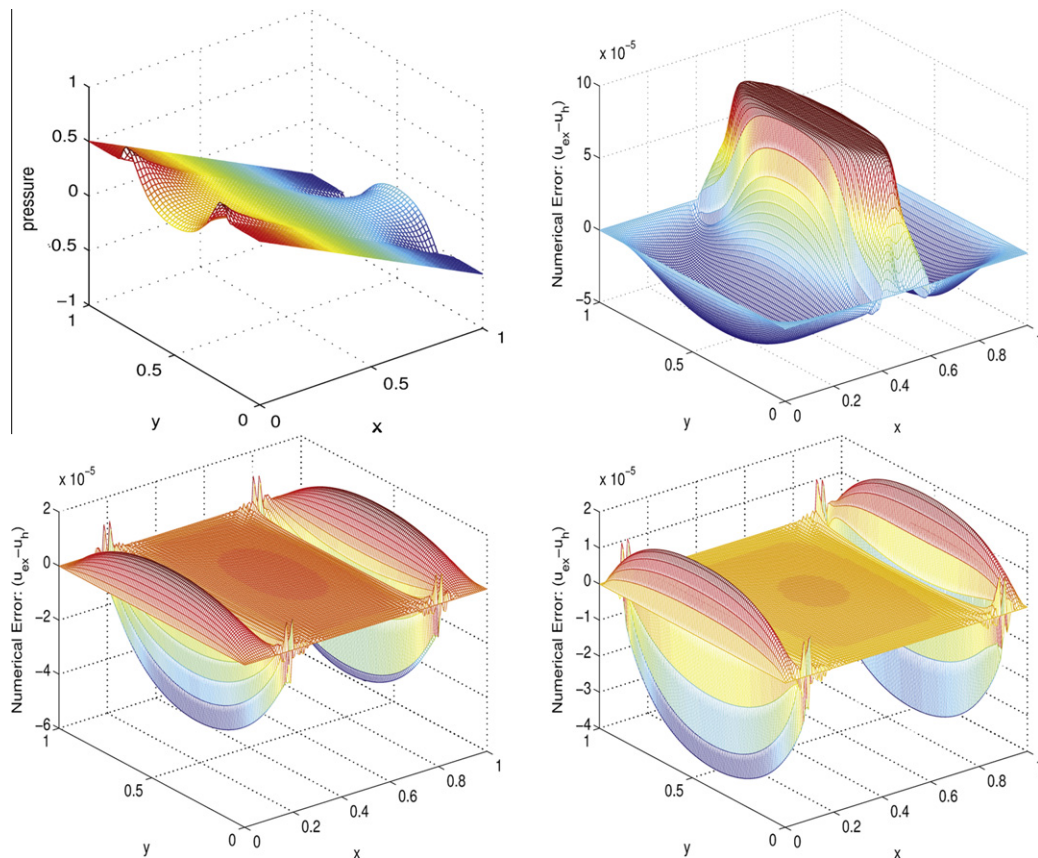


Fig. 6.2. Top, left: pressure field of the analytical test case computed with $\tau_s = 0.3$, $h = \frac{1}{128}$ and $\varepsilon = 10^{-5}$. Top, right: velocity error for $\tau_s = 0.1$. Bottom, velocity error for $\tau_s = 0.3$ and $\tau_s = 0.4$.

der-determined in the rigid region. The other subplots of the Figure illustrate the velocity error for different values of τ_s , pointing out the presence of error spikes in the neighborhood of the rigid region. Note however that the maximum error is of the order of 10^{-5} .

6.1.2. The lid-driven cavity

We perform two different numerical simulations, both of them in the unit square domain $\Omega = [0,1]^2$. For the first case, we solve (1.4) and (1.5) imposing Dirichlet boundary conditions by $\mathbf{u}|_{y=1} = (1,0)^T$ and $\mathbf{u} = \mathbf{0}$ everywhere else. Table 6.2 shows the number of iterations of the Picard method described in Section 3 for different sizes of the mesh and different values of τ_s and ε . Again, the comparison between the mixed formulation and the original one demonstrates the effectiveness of the former; for the primitive variables formulation the method does not converge within 500 iterations in some cases (denoted by -).

We compare also the numerical results of the mixed formulation with $\varepsilon = 0$ to the augmented formulation by Lions–Glowinski described in Section 5. The latter involves an additional parameter λ . In Fig. 6.3 on the left we compare the dynamics of the reduction of the difference $\|\tau^{(k+1)} - \tau^{(k)}\|$ along the iterations for several values of λ . The best choice for parameter λ is $\lambda = 0.01$.

Fig. 6.3 on the right illustrates the dynamics of $\|\tau^{(k+1)} - \tau^{(k)}\|$ along 200 iterations of the non-regularized version of (3.6), i.e. $\varepsilon = 0$ and the Lions–Glowinski method with $\lambda = 0.01$. Note that in the previous results we used the Picard residual for the stopping criterion, here we check the difference between two consecutive

computation of the stress. This is consistent with the common stopping criteria for the **ALG**. We used $\tau_s = 2$, $h = \frac{1}{32}$. The convergence rate of the mixed formulation is better than the one of the Lions–Glowinski formulation measured in terms of $\|\tau^{(k+1)} - \tau^{(k)}\|$ (notice however that Picard residual indicates the convergence to the same solution in less iterations). In general the identification of the optimal parameter λ is not easy whilst the solver for the new mixed formulation is parameter free.

Monitoring the difference $\|\gamma^{(k+1)} - \gamma^{(k)}\|$ we have obtained very similar results both for the convergence with different values of λ and the comparison with the mixed formulation (actually, with an even more evident better convergence rate for the mixed formulation), so we did not report the results here.

In the second experiment, we solve the unsteady Bingham problem taking into account the effect of the inertia terms, i.e. including the nonlinear convective term. We set the density $\rho = 1$ for simplicity. Unsteady problem in the mixed form reads

$$\begin{cases} \frac{\partial \mathbf{u}}{\partial t} + (\mathbf{u} \cdot \nabla) \mathbf{u} - \text{div} W + \nabla p = \mathbf{f}, \\ \nabla \cdot \mathbf{u} = 0, \\ W|_{Du} - Du = \mathbf{0}. \end{cases} \quad (6.2)$$

We impose Dirichlet boundary conditions by $\mathbf{u}|_{y=1} = (10,0)^T$ and homogeneous Dirichlet boundary conditions everywhere else. We choose $\Delta t = 0.1$ as the time step, $h = \frac{1}{128}$, $\varepsilon = 10^{-5}$ and $\tau_s = 2$ and $\mu = 0.1$. We solve the Stokes problem and the Navier–Stokes one. In Fig. 6.4 we show the Stokes and the Navier–Stokes solutions with

Table 6.2

Number of Picard iterations required for reducing the residual by 10^{-6} for the primitive variables formulation (left) and the mixed one (right) for the lid-driven cavity. For $h = 1/128$ and in many cases for $h = 1/64$ the iterations in primitive variables do not converge (-). The non-regularized case $\varepsilon = 0$ is included in the last column for the mixed formulation.

$h \downarrow \varepsilon \rightarrow$	10^{-1}	10^{-2}	10^{-3}	10^{-4}	10^{-5}	10^{-1}	10^{-2}	10^{-3}	10^{-4}	10^{-5}	0
	Primal					Dual					
$\tau_s = 2$:											
1 / 16	22	49	51	51	51	11	21	26	27	27	21
1 / 32	99	173	224	224	224	10	15	17	17	17	23
1 / 64	213	-	-	-	-	8	12	12	12	12	15
1 / 128	-	-	-	-	-	7	9	9	9	9	11
$\tau_s = 5$:											
1 / 16	18	37	48	51	51	17	31	37	37	38	27
1 / 32	66	94	269	267	266	14	22	23	24	24	32
1 / 64	128	-	-	-	-	12	17	18	18	18	22
1 / 128	-	-	-	-	-	10	13	14	14	14	15

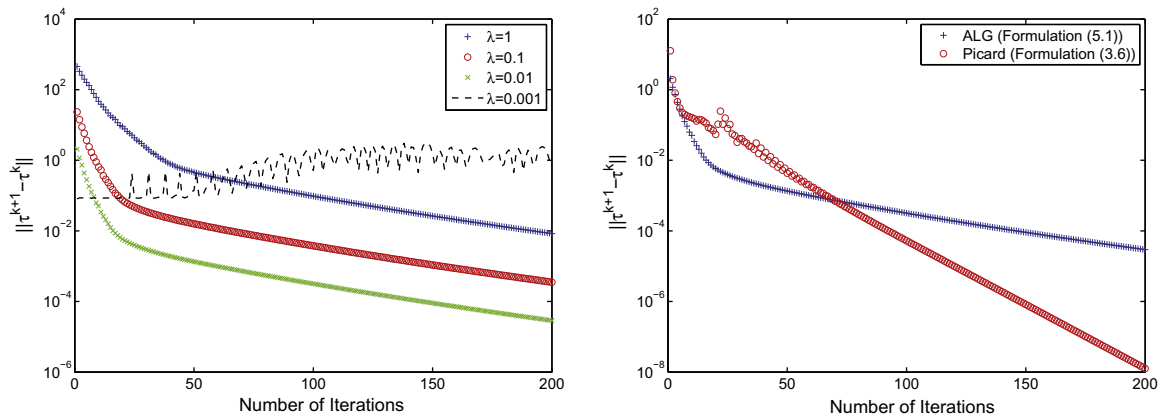


Fig. 6.3. Reduction of the difference $\|\tau^{k+1} - \tau^k\|$ for the first 200 iterations when solving the lid-driven cavity problem with $\tau_s = 2$ and $h = \frac{1}{32}$. Left: ALG with different choices of λ . No convergence occurs for the case of $\lambda = 0.001$. Right: Comparison between Picard iterations (3.6) with $\varepsilon = 0$ and formulation (5.1) with the algorithm ALG and $\lambda = 0.01$.

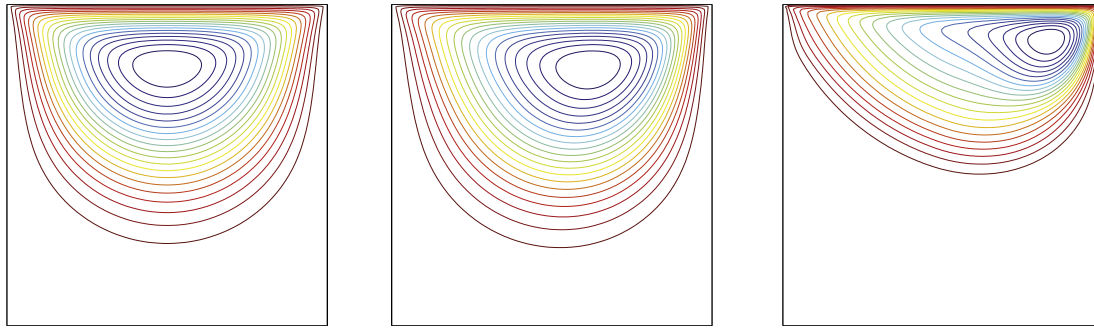


Fig. 6.4. Streamlines of the lid-driven cavity flow ($\tau_s = 2$, $h = \frac{1}{128}$ and $\varepsilon = 10^{-5}$). Left: Solution of the Stokes problem. Center and right: solution of the unsteady Navier–Stokes-type problem computed with $\mathbf{u}|_{y=1} = (10, 0)^T$, $\mu = 0.1$ (center) and $\mu = 0.01$ (right).

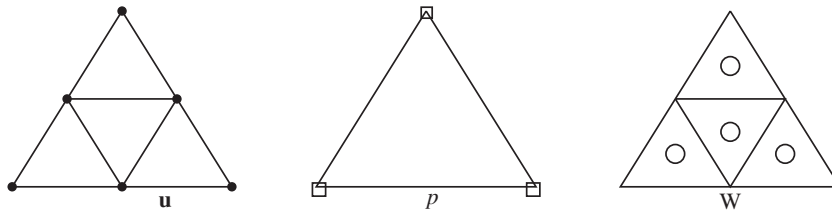


Fig. 6.5. Degrees of freedom for the $P^1_{\text{iso}}P^2-P^1-P^0_{\text{iso}}P^2$ elements used for the mixed formulation. \bullet are the degrees of freedom for the velocity components, \square for the pressure, \circ for the auxiliary tensor W .

```

 $\varepsilon_{\text{new}} := \varepsilon_{\text{curr}} := 0.1; \rho = 0.5;$ 
 $\mathbf{u} := \mathbf{u}_{\text{Stokes}}; p := p_{\text{Stokes}}; W := 0;$ 
while  $\varepsilon_{\text{curr}} > \varepsilon_{\text{target}}$ 
  [ $\mathbf{u}_{\text{new}}, p_{\text{new}}, W_{\text{new}}, \text{success}$ ]:=newton( $u, p, W, f, \varepsilon_{\text{curr}}$ )
  if (success==true) then
     $\varepsilon_{\text{new}} := \varepsilon_{\text{curr}}; \varepsilon_{\text{curr}} := \rho \varepsilon_{\text{curr}}; \rho = 0.9\rho;$ 
     $\mathbf{u} := \mathbf{u}_{\text{new}}; p = p_{\text{new}}; W := W_{\text{new}};$ 
  else
     $\rho := \frac{1 + \rho}{2}; \varepsilon_{\text{curr}} := \rho \varepsilon_{\text{new}};$ 
  end
end
    
```

Fig. 6.6. Pseudocode for the continuation algorithm with the Newton method. newton($\mathbf{u}, p, W; \mathbf{f}; \varepsilon_{\text{curr}}$) stands for one iteration of the Newton method; “success” == “true” if the new residual is less than $\varepsilon_{\text{curr}}$.

$\mu = 0.1$ and $\mu = 0.01$. The nonlinear term is handled with a linearization through a semi-implicit time advancing scheme. Effectiveness of the mixed formulation is confirmed also in this case. Plots of the solution in Fig. 6.4 show the equally distributed velocity streamlines at $t = 1$ after the solutions reached steady states.

6.2. Newton method with continuation, triangular elements

In this section, we show results of several numerical experiments with the Newton method enhanced by a continuation algorithm. We run tests for both primitive variables and mixed form of the discrete problem. These numerical results were produced using the different triple of finite element pairs: $P^1_{\text{iso}}P^2-P^1$ for velocity and pressure (\mathbf{V}_h consists of continuous piecewise linear functions with respect to the triangulation built by connecting the middle

points of the edges of the original triangulation), \mathcal{W}_h consists of piecewise constant functions with respect to the same refined triangulation (by analogy we will denote this element by $P^0_{\text{iso}}P^2$), cf. Fig. 6.5. Further in the tables, h denotes the size of the (larger) pressure element. Despite of a low approximation order, this choice of finite element spaces has several advantages: (i) \mathbf{V}_h and Q_h form an LBB stable pair, (ii) it holds $D(\mathbf{V}_h) \subset \mathcal{W}_h$, (iii) for any $\mathbf{u}_h \in \mathbf{V}_h$ and $W_h \in \mathcal{W}_h$ it holds $|D\mathbf{u}_h|_{\varepsilon} W_h \in \mathcal{W}_h$. Therefore (4.1) implies $|D\mathbf{u}_h|_{\varepsilon} W_h = D\mathbf{u}_h$ to be valid in a usual pointwise sense. Thus $P^1_{\text{iso}}P^2-P^1-P^0_{\text{iso}}P^2$ is a (somewhat exceptional) example of a stable FE triple which provides the *the equivalence of the discrete primitive variables and mixed formulations*, similar to their continuous counterparts. Thus, the difference between the two formulations lies entirely in the performance of the Newton type solvers, while the resulting discrete solution accuracy is the same. We also

Table 6.3

Total number of the Newton iterations within the continuation algorithm for the lid-driven cavity problem with $\varepsilon_{\text{target}} = 1e - 5$, $\tau_s = 2$, and varying h .

h	$\frac{1}{32}$	$\frac{1}{64}$	$\frac{1}{128}$	$\frac{1}{256}$
Primal form	95	104	107	
Augmented form	14	15	15	15
$-\psi_{\text{min}}$	0.08070	0.08182	0.08231	0.08254

Table 6.4

Total number of the Newton iterations within the continuation algorithm for the lid-driven cavity problem with $\varepsilon_{\text{target}} = 1e - 5$ and varying τ_s ; $h = \frac{1}{128}$.

τ_s	2	5	10
Primal form	107	123	140
Augmented form	14	29	46
$-\psi_{\text{min}}$	0.08231	0.06874	0.05696
y_{ψ}	0.805	0.836	0.861

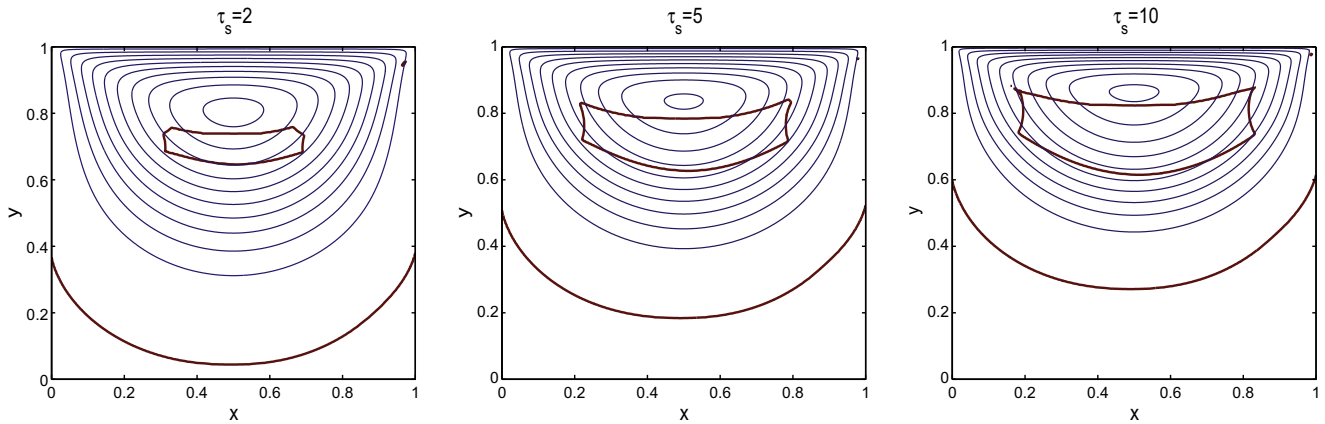


Fig. 6.7. Velocity streamlines (blue) and predicted yield surfaces (brown) of the lid-driven cavity flow computed for different values of the stress yield τ_s , with $h = \frac{1}{64}$. (For interpretation of the references to colour in this figure legend, the reader is referred to the web version of this article.)

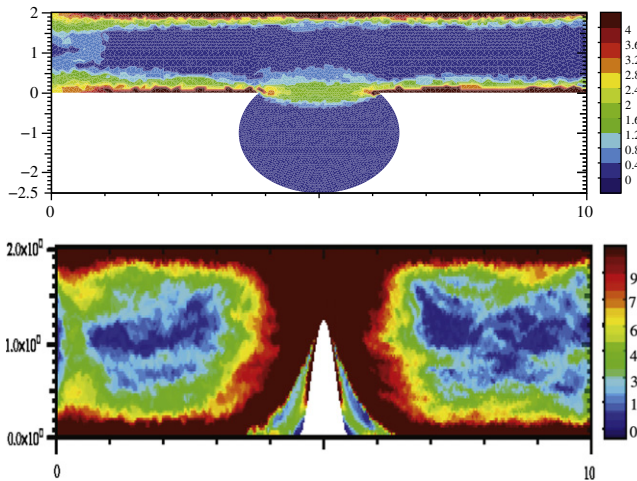


Fig. 6.8. Plot of $|Du|$ for a nontrivial domains with a circular cavity attached to a rectangular pipe (top) and an occluded pipe (bottom). Results obtained with the mixed non-regularized formulation.

remark that due to inherent irregularity of the visco-plastic solutions⁴ it may not be beneficial to use high order elements.

A pseudocode of the continuation algorithm we used is shown in Fig. 6.6. Newton iterations inside the continuation method are stopped (with “success” == “true”) once the L^2 norm of the nonlinear residual is less than ε , where ε is a current value of the regularization parameter. Numerical experiments show that finding \mathbf{u}_{new} , p_{new} , W_{new} with better accuracy does not lead to a better convergence of the subsequent Newton step. If during the `newton(...)` step the residual exceeds twice the initial residual (it was found beneficial to allow a small increase of residual on the first step of the Newton method), then the Newton iterations are terminated with “success” == “false”. The target ε in all our tests is 10^{-5} . On every step of the Newton method a linear system of algebraic equations was solved approximately by a preconditioned GMRES method. For these inner linear iterations the stopping criteria was the reduction of the initial residual by a factor of 0.1ε . Increasing the inner tolerance did not lead to a notable reduction of the total number of nonlinear iterations. We note again that for small

⁴ The velocity gradient is expected to have a kink on the yield surface, as clearly seen from the analytical example in (6.1), thus $\mathbf{u} \notin \mathbf{H}^3$. Of course, introducing $\varepsilon > 0$ smears the irregularity.

values ε the linear systems become increasingly ill-conditioned (for both primitive variables and mixed form) and special preconditioned iterative method should be developed to solve them efficiently. Lacking such solvers in our current implementation prevented us from decreasing $\varepsilon_{\text{target}}$ in this test below 10^{-5} .

Tables 6.3 and 6.4 show the total number of Newton iterations within the continuation algorithm (the total number includes also those iterations which were not accepted, i.e. ended with “success” = “false”). The results are shown for the problem in both primitive variables and the mixed form for different values of mesh size and stress yield. We also show the minimum of the stream function and the position of the main vortex center for the computed solutions. Fig. 6.7 presents the equally distributed velocity streamlines and the isoline of $(2\mu + \tau_s |Du|^{-1}) |Du| = \tau_s$, the latter may be interpreted as a reasonable approximation of the yield surfaces [35]. Comparing these statistics to those found in [29,30] we assure that sufficiently accurate solutions are computed.

6.3. A 2D computation on non-rectangular domains

We finally present two simple test cases carried out in non-rectangular geometries, showing that the mixed formulation even with no regularization is a viable approach for more realistic problems. Simulations are carried out with the code `FreeFem++` (version 3.9), P1 bubble finite elements for the velocity, P1 for the pressure and each component of the tensor W . A streamline upwind Petrov–Galerkin stabilization has been added for the treatment of the convective term (linearized with a Picard approach). In the first case we simulated a 2D circular cavity problem attached to a 2D rectangular channel. In the second case we considered a rectangular channel featuring an obstacle represented by a sinusoidal bump. We tested several values of the parameters, both the physical and the numerical ones. In particular, in Fig. 6.8 – left – we show the computed shear rate for the first geometry with $\tau = 1$, $\mu = 0.05$ and an incoming velocity profile with peak $u_M = 2$. In Fig. 6.8 – right – we present results for the second geometry with $\tau = 1$, $\mu = 0.1$, $\tau = 2$ and $u_M = 10$. The non-regularized mixed formulation gets convergent results also in these cases.

7. Conclusion

In this paper we introduced a new formulation for the regularized Bingham flow equations. This formulation has the advantage of being numerically more robust when the regularization parameter ε gets smaller. We proved well-posedness results for

the weak form of the problem and discussed algebraic properties of the discretized equations. We have performed several numerical experiments using finite element methods. These experiments show that the number of nonlinear iterations is significantly reduced for the new formulation compared to the classical formulation in primitive variables. The mixed formulation does not become singular in the plug region, so that, even if the theory of this paper covers only the regularized case, numerical experiments also demonstrate good performances for the non-regularized case. For the non-regularized case the mixed formulation was found to compare favorably to the classical Uzawa method based on the Lions-Glowinski approach. Further we plan to validate and use the new formulation for more practical 3D problems. Validation will include the accurate computation of the plug region in problems of practical interest (see [35]).

References

- [2] I.V. Basov, V.V. Shelukhin, Nonhomogeneous incompressible Bingham viscoplastic as a limit of nonlinear fluids, *J. Non-Newton. Fluid Mech.* 142 (2007) 95–103.
- [4] M. Bercovier, M. Engelman, A finite element method for incompressible non-Newtonian flows, *J. Comput. Phys.* 36 (1980) 313–326.
- [5] L.C. Berselli, L. Diening, M. Ruzicka, Existence of Strong Solutions for incompressible fluids with shear dependent viscosities, *J. Math. Fluid Mech.* 12 (1) (2010) 101–132.
- [6] R. Byron-Bird, G.C. Dai, B.J. Yarusso, The Rheology and Flow of Viscoplastic Materials, *Rev. Chem. Eng.* 1 (1) (1983) 2–70.
- [7] J. Cea, R. Glowinski, Méthodes numériques pour l'écoulement laminaire d'un fluide rigide visco-plastique incompressible, *Int. J. Comput. Math. Sec. B* 3 (1972) 225–255.
- [11] T. Chan, G. Golub, P. Mulet, A nonlinear primal-dual method for total variation-based image restoration, *SIAM J. Sci. Comput.* 20 (6) (1999) 1964–1977.
- [12] E.J. Dean, R. Glowinski, Operator-splitting methods for the simulation of Bingham visco-plastic flow, *Chin. Ann. Math.* 23 (2002) 187–204.
- [13] E.J. Dean, R. Glowinski, G. Guidoboni, On the numerical simulation of Bingham visco-plastic flow: old and new results, *J. Non-Newton. Fluid Mech.* 142 (2007) 36–62.
- [15] G. Duvaut, J.L. Lions, *Inequalities in Mechanics and Physics*, Springer, 1976.
- [16] L.C. Evans, *Partial Differential Equations*, Graduate Studies in Mathematics, vol. 19, Springer, 1998.
- [17] H. Elman, D. Silvester, A. Wathen, *Finite Elements and Fast Iterative Solvers with Applications in Incompressible Fluid Dynamics*, Oxford University Press, 2005.
- [18] I.A. Frigaard, C. Nouar, On the usage of viscosity regularization methods for viscoplastic fluid flow computation, *J. Non-Newton. Fluid Mech.* 127 (2005) 1–26.
- [19] I.A. Frigaard, G. Ngwa, O. Scherzer, On effective stopping time selection for visco-plastic nonlinear BV diffusion filters used in image denoising, *SIAM J. Appl. Math.* 63 (6) (2003) 1911–1934.
- [20] I.A. Frigaard, O. Scherzer, Herschel–Bulkley diffusion filtering: non-Newtonian fluid mechanics in image processing, *Z. Angew. Math. Mech.* 86 (6) (2006) 474–494.
- [23] V. Girault, P.A. Raviart, *Finite element methods for Navier–Stokes equations: theory and algorithms*, Springer Series in Computational Mathematics, vol. 5, Springer, Verlag, 1986.
- [24] R. Glowinski, *Numerical Methods for Nonlinear Variational Problems*, Springer, Verlag, New York, NY, 1984.
- [25] P.P. Grinevich, M.A. Olshanski, An iterative method for the stokes-type problem with variable viscosity, *SIAM J. Sci. Comput.* 31 (5) (2009) 3959–3978.
- [26] J. Hron, A. Ouazzi, S. Turek, A Computational Comparison of two FEM Solvers For Nonlinear Incompressible Flow, *Challenges in Scientific Computing*, Springer, 2004.
- [27] E.A. Muravleva, M.A. Olshanskii, Two finite-difference schemes for the calculation of Bingham fluid flows in a cavity, *Russ. J. Numer. Anal. Math. Model.* 23 (6) (2008) 615–634.
- [29] E. Mitsoulis, Th. Zisis, Flow of Bingham plastics in a lid-driven cavity, *J. Non-Newton. Fluid Mech.* 101 (2001) 173–180.
- [30] M.A. Olshanskii, Analysis of semi-staggered finite-difference method with application to Bingham flows, *Comput. Methods Appl. Mech. Eng.* 198 (2009) 975–985.
- [31] H. Schmitt, Numerical simulation of Bingham fluid flow using prox-regularization, *J. Optim. Theory Appl.* 106 (3) (2000) 603–626.
- [32] T.C. Papanastasiou, Flows of materials with yield, *J. Rheol.* 31 (1987) 385–404.
- [34] N. Roquet, P. Saramito, An adaptive finite element method for Bingham fluid flows around a cylinder, *Comput. Methods Appl. Mech. Eng.* 192 (31–32) (2003) 3317–3341.
- [35] A. Putz, I.A. Frigaard, D.M. Martinez, On the Lubrication Paradox and the use of Regularisation Methods for Lubrication Flows, *Journal of Non-Newtonian Fluid Mechanics*, Elsevier, 2009.
- [36] M. Sahin, H.J. Wilson, A semi-staggered dilation-free finite volume method for the numerical solution of viscoelastic fluid flows on all-hexahedral elements, *J. Non-Newton. Fluid Mech.* 147 (2007) 79–91.
- [37] A.M. Robertson, A. Sequeira, V. Kameneva, in: G.P. Galdi, R. Rannacher, A.M. Robertson, S. Turek (Eds.), *Hemorheology in Hemodynamical Flows*, Birkhauser, Basel, 2008.
- [38] G. Vinay, A. Wachs, J.F. Agassant, Numerical simulation of weakly compressible Bingham flows the restart of pipeline flows of waxy crude oils, *J. Non-Newton. Fluid Mech.* 136 (2–3) (2006) 93–105.
- [39] G. Vinay, A. Wachs, I. Frigaard, Start-up transients and efficient computation of isothermal waxy crude oil flows, *J. Non-Newton. Fluid Mech.* 143 (2–3) (2007) 141–156.